Oceanologia 65 (2023) 571—594

Available online at www.sciencedirect.com

ScienceDirect

journal homepage: www.journals.elsevier.com/oceanologia

ORIGINAL RESEARCH ARTICLE

Dinoflagellate cysts and benthic foraminifera from surface sediments of Svalbard fjords and shelves as paleoenvironmental indicators

Maciej M. Telesiński[a,*], **Vera Pospelova**[b], **Kenneth Neil Mertens**[c], **Małgorzata Kucharska**[a], **Marek Zajączkowski**[a]

[a] *Institute of Oceanology, Polish Academy of Sciences, Sopot, Poland*
[b] *University of Minnesota, Department of Earth and Environmental Sciences, College of Science & Engineering, Minneapolis, USA*
[c] *LITTORAL, Ifremer, Concarneau, France*

Received 6 October 2022; accepted 14 June 2023
Available online 28 June 2023

KEYWORDS
North Atlantic;
Nordic Seas;
Sea ice;
Primary productivity;
Fjords;
Sediments;
Chlorophyll-*a*

Abstract Due to the Arctic amplification effect, the Svalbard archipelago is an important area for studying ongoing environmental changes. However, its marine ecosystem is extremely complex. In this study, we analyze modern assemblages of dinoflagellate cysts (dinocysts) and benthic foraminifera from surface sediment samples around Svalbard. We use multivariate statistical analyses to examine relationships between environmental conditions (summer and winter sea surface temperature and salinity, sea-ice cover, etc.) and both microfossil groups to evaluate their use as proxies for reconstructions of the marine environment in the region. Our results show that the most important factor controlling the environment around Svalbard is the Atlantic Water which mostly impacts the western coast, but its influence reaches as far as the eastern coast of Nordaustlandet. However, on a local scale, such factors as the sea-ice cover, the presence of tidewater glaciers, or even the morphology and hydrology of fjords become increasingly important. We found that two dinocyst species, cysts of *Polarella glacialis* and *Echinidinium karaense*, can be considered regional winter drift ice indicators. The relationships between environmental parameters and benthic foraminiferal assemblages are much more difficult to interpret. Although statistical analysis shows a correlation of benthic foraminiferal species with various environmental parameters, this correlation might be some-

* Corresponding author at: Institute of Oceanology Polish Academy of Sciences, Powstańców Warszawy 55, Sopot 81—712, Poland.
E-mail address: mtelesinski@iopan.pl (M.M. Telesiński).
Peer review under the responsibility of the Institute of Oceanology of the Polish Academy of Sciences.

Production and hosting by Elsevier

https://doi.org/10.1016/j.oceano.2023.06.007

what coincidental and caused by other factors not analyzed in this study. Nevertheless, the use of two complementary microfossil groups as (paleo)environmental indicators can provide a more comprehensive picture of the environmental conditions.

List of abbreviations

AF	Arctic Front
AW	Atlantic Water
ArW	Arctic Water
dinocysts	dinoflagellate cysts
ESC	East Spitsbergen Current
NAC	North Atlantic Current
SSS	sea surface salinity
SST	sea surface temperature
TAW	Transformed Atlantic Water
WCW	Winter-cooled Water
WSC	West Spitsbergen Current

List of taxa (mentioned in the text)

Dinoflagellate cysts:
Ataxiodinium spp.
Cysts of *Biecheleria* cf. *baltica*
Brigantedinium spp.
Dubridinium spp.
Echinidinium karaense
Echinidinium spp.
Islandinium? *cezare*
Islandinium minutum
Nematosphaeropsis labyrinthus
Operculodinium centrocarpum sensu Wall and Dale (1966)
Cysts of *Pentapharsodinium dalei*
Cysts of *Polarella glacialis*
Cysts of *Protoperidinium nudum*
RBC, round brown cyst
SBC, spiny brown cyst
Selenopemphix quanta
Spiniferites elongatus
unidentified 1 & 2
Foraminifera:
Adercotryma glomeratum
Buccella frigida
Cassidulina reniforme
Cibicides lobatulus
Elphidium clavatum
Globobulimina arctica-turgida
Islandiella helenae
Islandiella norcrossi
Labrospira crassimargo
Melonis barleeanus
Nonionellina labradorica
Portatrochammina karica
Recurvoides turbinatus
Reophax scorpiurus
Spiroplectammina spp.
Stainforthia loeblichi
Textularia earlandi-kattegatensis
Trifarina fluens

1. Introduction

The Svalbard archipelago is one of the crucial areas to study ongoing global warming. First of all, it is located in high northern latitudes where any environmental changes can be easily observed due to the Arctic amplification effect (e.g., Balazy and Kuklinski, 2019; Schiermeier, 2007; Serreze and Barry, 2011; Serreze and Francis, 2006). Secondly, the archipelago constitutes a frontal area between relatively warm Atlantic waters and cold, sea ice-bearing Arctic waters, which enables the study of the influence of their interplay on both terrestrial and marine environments, especially in numerous fjords cutting deep into landmasses and creating a unique interface between the land and the sea (e.g., Cottier et al., 2005; Syvitski and Shaw, 1995). The effect of sea ice is particularly important as the sea ice-albedo feedback is thought to be associated with a decrease in the snow and ice cover and a corresponding increase in the surface temperature, further decreasing the snow and ice cover. It is shown that the sea ice-albedo feedback can operate even in multiyear pack ice, without the disappearance of this ice, associated with internal processes occurring within the multiyear ice pack (e.g., duration of the snow cover, sea-ice thickness and distribution, lead fraction, and melt pond characteristics) (Curry et al., 1995). The presence of ice caps and glaciers, including tidewater ice margins (e.g., Dowdeswell, 1989), is another characteristic feature of Svalbard allowing the investigation of feedback between land-based ice masses and the ocean. Finally, Svalbard's relative ease of access, compared to other Arctic regions, makes it one of the most important natural Arctic laboratories concentrating scientific efforts of a wide range of disciplines.

To understand modern changes in the environment, studies of its natural variability reaching beyond historical observations are necessary. Remains of microorganisms are often used in paleoceanographic reconstructions as they are usually abundant in marine sediments and provide information on numerous parameters of the environment in which they lived. Unfortunately, in the Svalbard fjords, some microfossil groups like planktic foraminifera or diatoms are absent or have a poor fossil record which limits the possibilities of (paleo)environmental studies (e.g., Korsun et al., 1995; Zgrundo et al., 2017). On the other

hand, fjords in the region are described as "hot spots" for other microfossil groups such as dinoflagellate cysts (e.g., Grøsfjeld et al., 2009; Howe et al., 2010) and benthic foraminifera (e.g., Pawłowska et al., 2017; Szymańska et al., 2021).

Dinoflagellates are a major group of microscopic plankton commonly found in marine environments (e.g., Taylor et al., 2008; Zonneveld et al., 2013). This group is very diverse in coastal waters, and about half of the dinoflagellates are phototrophic (commonly called autotrophic) and directly contribute to marine primary productivity, whereas the other half is heterotrophic, i.e., feeding on a wide range of microorganisms, including diatoms and small flagellates (e.g., Jacobson and Anderson, 1996; Jeong, 1999; Taylor, 1987). Mixotrophy among dinoflagellates is now known to be widespread (e.g., Stoecker, 1999). In the fossil record, dinoflagellates are represented by their resting stages called cysts, generally produced during the sexual reproduction phase (e.g., Dale, 1983; Taylor, 1987). Dinoflagellate cysts (dinocysts) have organic walls that are highly resistant to physical, chemical, and biological degradation and can be preserved in sediments for hundreds of millions of years (e.g., Dale, 1996; Fensome et al., 1993). Dinocyst diversity, relative and absolute abundances, and the presence of specific taxa in sediments encode information about some of the dinoflagellate populations in the upper water column and, thus, environmental factors that influence their distributions (e.g., Dale, 1976; Zonneveld et al., 2013). Biogeographical distribution of dinocysts has been widely documented over the years (e.g., Dale, 1996) and it demonstrated that these microfossils can be successfully used for qualitative and quantitative reconstructions of sea-surface temperature (SST), salinity (SSS), primary productivity, coastal eutrophication, and pollution in the Late Quaternary (e.g., Dale, 2009; Dale and Dale, 2002). Furthermore, the sea-ice cover appears to be another driving factor in cyst distributions in high latitudes, and some taxa have affinities for polar environments and are potential sea-ice indicators (e.g., de Vernal et al., 2020, 2013, 2001; de Vernal and Marret, 2007; Marret et al., 2020; Matthiessen et al., 2005; Obrezkova et al., 2023; Rochon et al., 1999). The seafloor sediments of areas characterized by multiyear perennial pack-ice are usually barren of dinocysts (e.g., de Vernal et al., 2020, 2005, 2001). Nevertheless, there are a few dinocyst taxa that are known to occur in sediments of areas marked by seasonal sea ice and even in high abundances (e.g., Grøsfjeld et al., 2009; Harland, 1982; Head et al., 2001; Heikkilä et al., 2014; Howe et al., 2010; Mudie and Rochon, 2001; Zonneveld et al., 2013). Neritic settings of Arctic seas with seasonal sea ice are usually characterized by *Islandinium minutum*, *Islandinium*? *cezare*, *Echinidinium karaense* and *Polykrikos*? sp. — Arctic morphotypes, whereas dinocyst assemblages from offshore regions have high abundances of *Impagidinium pallidum* and *Spiniferites elongatus* (e.g., de Vernal et al., 2020). Only a few cyst-forming species are known to dwell in the ice-pack environment. The most common examples are cysts of *Polarella glacialis* which were first described from sea-ice brine channels in Antarctica (Montresor et al., 1999) and the Canadian Arctic (Montresor et al., 2003).

Another key group of microorganisms thriving in Svalbard fjords and shelves with high biodiversity are benthic foraminifera (e.g., Murray, 1991). Their short life cycle and sexual reproduction allowing high genetic changeability make them good bioindicators for both short- and long-term environmental changes on a local as well as global scale (e.g., Barbieri et al., 2006). Due to the high preservation potential of the foraminiferal tests in sediment, they can be used as a proxy to reconstruct paleoenvironmental changes such as water temperature, salinity as well as oxygen and nutrients availability (e.g., Hald et al., 2001; Ślubowska et al., 2005). Benthic foraminiferal distribution in Svalbard fjords is conditioned by environmental gradients (e.g., Jernas et al., 2018). Close to tidewater glaciers, the conditions are unstable and the foraminiferal assemblages are characterized by low abundance and dominance of a few opportunistic species. In the outer parts of fjords, the conditions are more stable allowing for higher abundance and diversity of foraminiferal assemblages as well as a higher percentage of Atlantic Water-related species (Fossile et al., 2022; Hald and Korsun, 1997; Hansen and Knudsen, 1995; Jima et al., 2021; Korsun et al., 1995; Korsun and Hald, 2000; Kucharska et al., 2019; Mackensen et al., 2017; Majewski and Zajączkowski, 2007; Włodarska-Kowalczuk et al., 2013; Zajączkowski and Włodarska-Kowalczuk, 2007). As the water temperature is one of the main abiotic factors controlling benthic foraminifera distribution (e.g., Murray and Alve, 2016) it is important to study changes in benthic foraminiferal assemblages in the face of ongoing oceanographic and climatic changes.

In this study, we analyze modern assemblages of both dinocysts and benthic foraminifera and their relationships with environmental conditions to evaluate their use as proxies for reconstructions of the marine environment in Svalbard fjords and surrounding coastal waters. Although both groups have great potential to be used as bioindicators for modern and past environments, when combined, they can provide an even more complete image of the marine environment around Svalbard. We analyze the relationships between the two groups and surface water parameters, such as the dominant water masses, temperature and salinity, and sea-ice occurrence. We decided to focus only on surface water conditions, as these are available over extended periods of time from satellite observations. Even though surface water parameters might not influence benthic foraminiferal assemblages in a straightforward way, they certainly influence them indirectly, e.g., by regulating the food flux reaching the bottom.

2. Study area and oceanographic conditions

The Svalbard archipelago is influenced by two main water masses, Atlantic Water (AW) and Arctic Water (ArW). The relatively warm and saline AW ($T > 3°C$, $S > 34.65$, Cottier et al., 2005) is transported by the West Spitsbergen Current (WSC), the northernmost branch of the North Atlantic Current (Figure 1). Its flow is mainly confined to the continental slope (e.g., Saloranta and Svendsen, 2001), although the expansion of AW across the shelf and into the fjords, mostly below a 20—30 m thick surface layer (Figure 2A), occurs frequently (e.g., Cottier et al., 2005; Nilsen et al., 2016, 2008) as also confirmed by our CTD measurements (Figure 2). North of Svalbard, the WSC splits

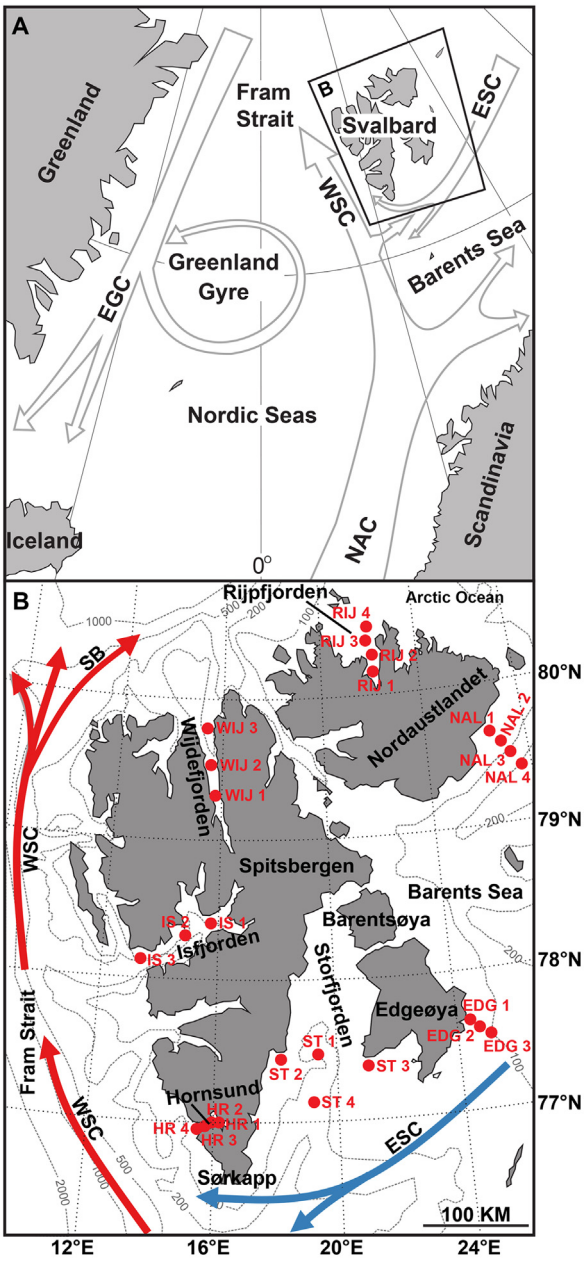

Figure 1 Location map showing the present-day surface water circulation (A) in the Nordic Seas and (B) around Svalbard. Positions of sampled stations are marked with red dots. Red arrows indicate AW, blue arrows — ArW. The surface currents are: EGC — East Greenland Current; ESC — East Spitsbergen Current; NAC — North Atlantic Current; SB — Svalbard branch of the WSC; WSC — West Spitsbergen Current.

into three primary branches. The easternmost Svalbard branch of the WSC encompasses the northern coasts of the archipelago (Aagaard et al., 1987) and represents the largest input of AW into the Arctic Ocean (Manley, 1995). The relatively cold and less saline ArW ($-1.5°C < T < 1°C$, $34.3 < S < 34.8$, Cottier et al., 2005) is transported from the northeast by the East Spitsbergen Current (ESC), together with drift ice from the Barents Sea (e.g., Saloranta and Svendsen, 2001; Skogseth et al., 2005). ArW mostly influences the eastern and southern coasts of Svalbard, though even here traces of AW can be found (Figure 2D, F and G). After passing the Sørkapp, the ESC turns northward and continues along the Svalbard continental shelf where it is influenced by the outflow from the adjacent fjords (e.g., Cottier et al., 2005). The mixing of the two water masses (i.e. AW and ArW) on the shelf leads to the formation of Transformed Atlantic Water (TAW) ($1°C < T < 3°C$, $S > 34.65$, Cottier et al., 2005). Other water masses, such as Winter-Cooled Water (WCW), and Local Water are restricted to the inner parts of all Svalbard fjords.

Sea-ice conditions around Svalbard are strictly related to water mass dominance. On the western coast, where waters are generally warmer and saltier, pack ice (e.g., WMO, 2014) is rarely seen, especially during the last few years (e.g., Dahlke et al., 2020). An exception is the area near Sørkapp where the ESC often brings pack ice from the Barents Sea. On the other hand, the sea surface around the eastern and northern coasts of the archipelago is rarely ice-free even during summer as pack ice from the high Arctic is often drifting here with water masses from the north (e.g., Comiso, 2002). Fast ice forming during winter and melting in spring often occurs in the inner parts of Svalbard fjords (e.g., Fossile et al., 2020).

The study area includes seven locations around Svalbard — five fjords (Storfjorden, Hornsund, Isfjorden, Wijdefjorden and Rijpfjorden) and coastal zones of two ice-covered islands: Nordaustlandet and Edgeøya (Figure 1). Based on the general oceanography of the region, as well as on our CTD results, the locations can be divided into three major areas: AW-dominated (including Isfjorden, Wijdefjorden and Rijpfjorden), ArW-dominated (Storfjorden and Hornsund), and locally/glacier-influenced (Nordaustlandet and Edgeøya).

Isfjorden is the largest fjord system on Svalbard. It is located on the western coast of Spitsbergen and is orientated north-east to south-west. The fjord has a length of 70 km and a water depth of up to 425 m (e.g., Rasmussen et al., 2012). The Isfjorden system is widely open to the inflow of Transformed Atlantic Water (TAW, Figure 2A) from the shelf as it has no sill at its mouth (e.g., Nilsen et al., 2016). The sea-ice cover in Isfjorden is seasonal, i.e. all ice in the fjord melts during summer. Freezing usually starts in late November and lasts until mid-May. The ice cover normally consists of locally formed fast ice with some drift ice entering from the shelf areas. In the mouth area, the ice cover is normally weak or non-existent (e.g., Nilsen et al., 2008).

Wijdefjorden is a 110 km long, south-north oriented fjord, located on the northern coast of Spitsbergen (Figure 1). The fjord has its prolongation (without a threshold) as a wide depression on the shelf (Kowalewski et al., 1990). Two basins can be identified in the inner part of the fjord with maximum water depths of 245 m and 170 m (e.g., Hald and Korsun, 1997). Five glaciers are discharging into the fjord. Despite its northern location, this fjord is exposed to the influence of AW from the WSC (Figure 2B) (Loeng et al., 1997; Maslowski et al., 2004; Pfirman et al., 1994; Rudels et al., 1994; Rudels and Friedrich, 2000), while the analysis of ice charts indicates frequent presence of drift ice in the fjord (NMI Ice Services, http://cryo.met.no accessed on 19.01.2021).

Rijpfjorden is a north-facing fjord located on the northern coast of Nordaustlandet (Figure 1). The fjord has a max-

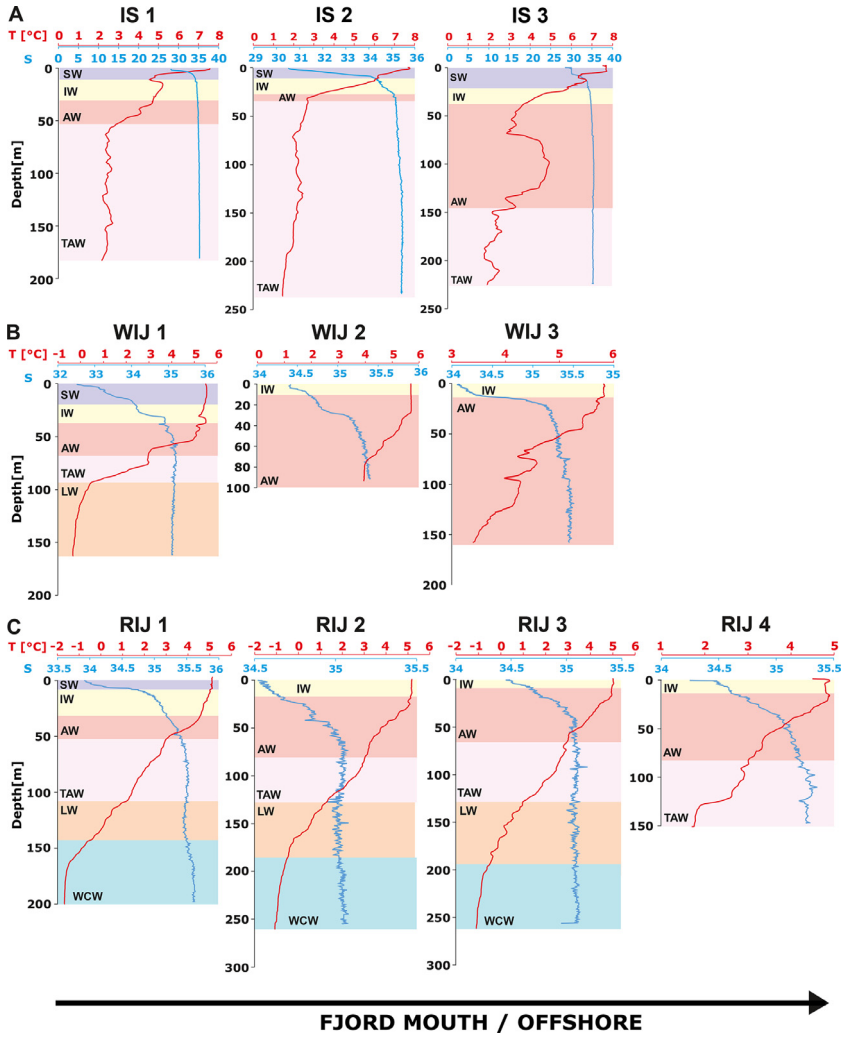

Figure 2 Water temperature [°C] (in red) and salinity (in blue) profiles measured at the sampling stations. Sampling dates are given in Table 1. Water masses at different depths are labelled (classification after Cottier et al., 2005). ArW — Arctic Water, AW — Atlantic Water, IW — Intermediate Water, LW — Local Water, SW — Surface Water, TAW — Transformed Atlantic Water, WCW — Winter-Cooled Water.

imum water depth of 270 m and is widely open towards the broad and shallow shelf (100—200 m deep). Rijpfjorden has generally been considered a 'true' Arctic fjord, as it was dominated by cold ArW, with a weak AW inflow. However, in recent years, the influence of AW has been steadily increasing (Figure 2C). In most years, sea ice lasts there from October until July (e.g., Ambrose et al., 2006; Søreide et al., 2010; Wallace et al., 2010) with some interannual variability in sea ice abundance and its thickness (Leu et al., 2011).

Nordaustlandet (Figure 1) is covered with the three main ice masses: Austfonna, Vestfonna, and Vegafonna (Dowdeswell and Drewry, 1985). Austfonna accounts for ~45% of the total calving flux from the Svalbard archipelago (Dowdeswell et al., 2008). The forefield of Austfonna is mostly covered with multiyear ice from the Arctic Ocean. Since the late 1970s, a progressive decrease in the sea-ice cover in the Barents Sea is observed (e.g., Comiso, 2002), causing an increase in moisture transport across Nordaustlandet and the growth of its ice masses (e.g., Bamber et al., 2004). The structure of the water column near the glaciated coastline is the result of the mixing of different water masses, including glacial meltwater. Further offshore, ArW becomes dominant. However, AW can also be traced (Figure 2D).

Edgeøya (Figure 1) is located on the eastern side of the Svalbard archipelago. It borders the Barents Sea to the east and Storfjorden to the west. In the north, the Freemansundet strait separates Edgeøya from Barentsøya. Edgeøya is covered by several glaciers, the largest of which is Edgeøyjøkulen on its eastern side. ArW dominance was observed close to the northeastern coast of Edgeøya, while AW was found beneath the surface layer of ArW off the southeastern coast (Carroll et al., 2008). Our CTD measurements confirm the dominance of ArW further offshore, while mixed water masses were identified closer to the coast. AW has not been traced (Figure 2E). Similar to Austfonna, mostly multiyear ice from the Arctic Ocean can be found off the eastern coast of Edgeøya.

Storfjorden is an approximately 190-km-long glacial trough that is enclosed by the landmasses of Spitsbergen to the west and Edgeøya and Barentsøya to the east and is

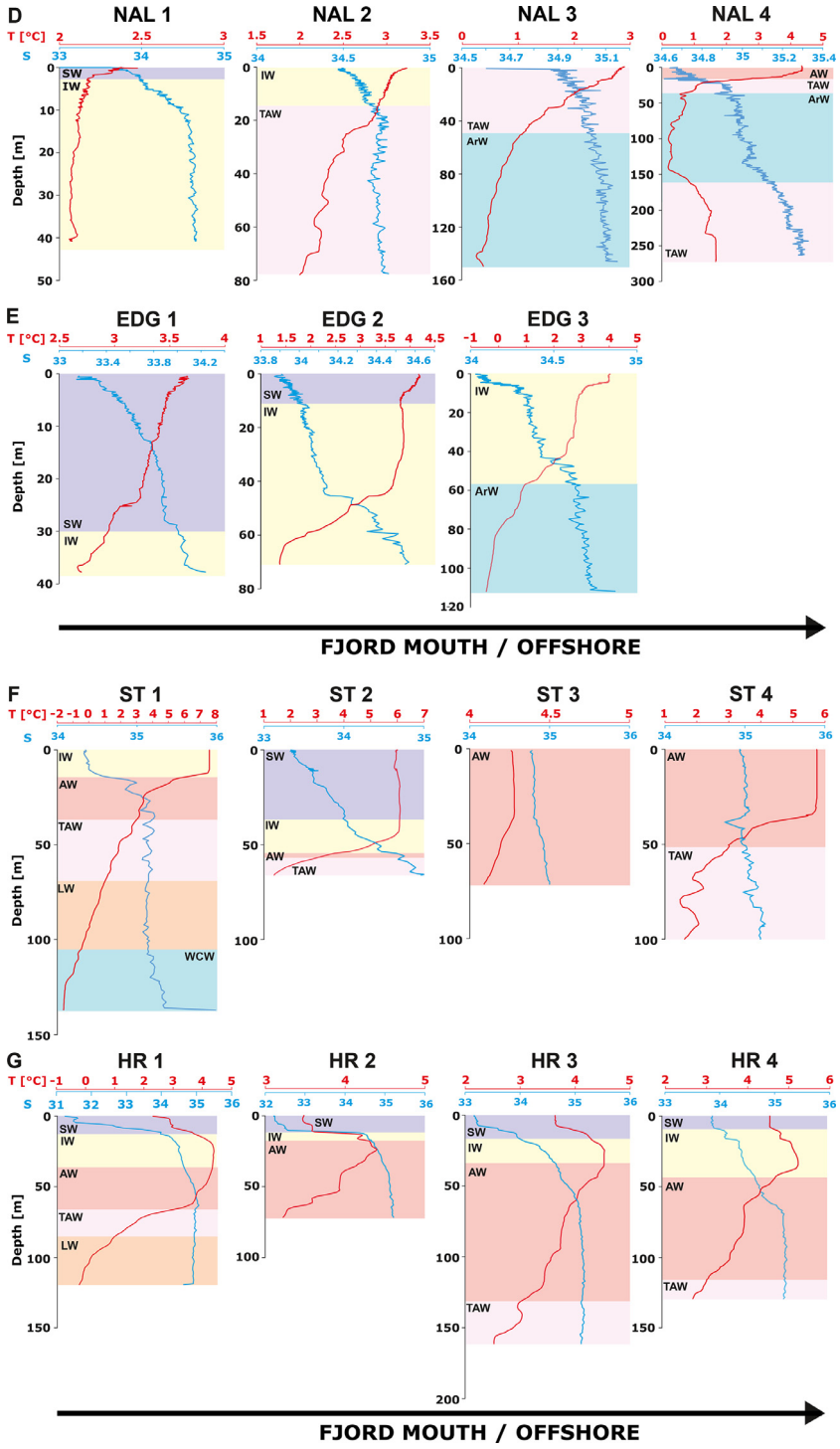

Figure 2 *Continued.*

limited by the shallow Storfjordbanken in the south-east. Storfjorden consists of two basins about 190 m deep, bordered by shallow (ca. 40 m) shelves. A 120-m deep sill crosses the mouth of Storfjorden at about 77°N and separates the main basin from Storfjordrenna, a continuation of the trough that extends beyond the shelf break (Skogseth et al., 2005). The water column in Storfjorden is composed of a mixture of two exogenous water masses and mixed waters that are formed locally (Figure 2F). ArW is transported by the ESC. AW, carried by the WSC, enters Storfjorden at a depth of 50—70 m (Akimova et al., 2011; Fer et al., 2003) though we have found it also on the surface. Brine-enriched shelf water is produced during sea-ice formation within the fjord (Haarpaintner et al., 2001; Skogseth et al., 2005, 2004). As fast ice forms in the inner part of Storfjorden starting in mid-November (Haarpaintner et al., 2001), the subsequently coming pack ice cannot enter the bay and is directed further towards Sørkapp and Hornsund.

Table 1 Sampling stations with their geographic position, water depth and sampling date.

Station	Latitude	Longitude	Depth [m]	Sampling date
Isfjorden				
IS 1	78°24.000′N	15°35.690′E	251	13.08.2016
IS 2	78°15.890′N	14°51.200′E	250	13.08.2016
IS 3	78°09.800′N	14°07.100′E	230	13.08.2016
Wijdefjorden				
WIJ 1	79°53.815′N	15°19.066′E	165	14.08.2016
WIJ 2	79°29.359′N	15°33.475′E	93	14.08.2016
WIJ 3	79°09.464′N	16°00.085′E	160	15.08.2016
Rijpfjorden				
RIJ 1	80°05.374′N	22°12.966′E	202	16.08.2016
RIJ 2	80°18.464′N	22°10.951′E	258	16.08.2016
RIJ 3	80°22.354′N	22°05.736′E	258	15.08.2016
RIJ 4	80°30.288′N	22°02.996′E	154	15.08.2016
Nordaustlandet				
NAL 1	79°42.727′N	26°34.955′E	43	18.08.2016
NAL 2	79°40.506′N	26°48.952′E	80	18.08.2016
NAL 3	79°36.241′N	27°30.196′E	147	18.08.2016
NAL 4	79°33.185′N	28°00.347′E	277	18.08.2016
Edgeøya				
EDG 1	77°42.925′N	24°12.853′E	41	19.08.2016
EDG 2	77°41.147′N	24°39.384′E	72	19.08.2016
EDG 3	77°39.751′N	25°00.162′E	112	19.08.2016
Storfjorden				
ST 1	77°27.163′N	19°14.230′E	251	14.08.2014
ST 2	77°24.138′N	17°51.734′E	67	14.08.2014
ST 3	77°14.728′N	20°53.185′E	72	15.08.2014
ST 4	76°53.181′N	19°27.559′E	158	14.08.2014
Hornsund				
HR 1	76°59.571′N	16°25.254′E	120	13.08.2014
HR 2	77°00.057′N	16°06.554′E	73	13.08.2014
HR 3	76°59.115′N	15°50.573′E	162	13.08.2014
HR 4	76°57.415′N	15°22.585′E	130	13.08.2014

Hornsund, the southernmost fjord of Svalbard (Figure 1), is 34 km long and 5—10 km wide. It is divided into several basins separated by sills with water depths usually over 100 m. The central basin is more than 250 m deep and the ice-proximal basins are 55-180 m deep (Zajączkowski et al., 2010). AW has been identified along the entire main axis of the fjord, below a ~40 m-thick layer of SW and IW (Figure 2G). Hornsund is the most 'glaciomarine' of the Spitsbergen fjords as almost 70% of the drainage area is covered by glaciers with thirteen tidewater glaciers entering the fjord (Błaszczyk et al., 2013; Hagen et al., 1993; Węsławski et al., 1991). Except for seasonal sea-ice cover in winter, Hornsund is often occupied by the pack ice brought there from the Barents Sea by the ESC in late spring and summer (e.g., Błaszczyk et al., 2013 and references therein; Węsławski et al., 1991).

3. Material and methods

3.1. Fieldwork

In total, 25 surface sediment samples were collected with a box corer (20 × 20 cm) for dinocyst analyses and with a small gravity corer (inner diameter 4.5 cm) for foraminiferal analyses during a cruise of r/v *Oceania*. Geographic positions, water depth, and sampling dates for each station are provided in Table 1. The samples were collected in August 2014 in Storfjorden (four stations; unfortunately, foraminiferal samples from station ST2 are missing) and Hornsund (four stations), and in August 2016 in Isfjorden (three stations), Wijdefjorden (three stations), Rijpfjorden (four stations) and in the coastal zones of Austfonna on Nordaustlandet (four stations) and Edgeøyjøkulen on Edgeøya (three stations, Figure 1). The temperature and salinity of the water column at each station were measured with a Mini CTD Sensordata SD202 at 1 s intervals. The depth of the water was measured with the hull-mounted echo sounder during sample retrieval.

3.2. Dinoflagellate cyst sample preparation and identification

The dinocyst analysis methodology used in this study is consistent with the standardized methodology described in Pospelova et al. (2005, 2010). The uppermost 2 cm of sediment from the box corer were collected into a zip bag and

stored at a temperature of −20°C. With recent accumulation rates along the main axes of Svalbard fjords (e.g., 0.5–0.7 cm y^{-1} in Hornsund, Glud et al., 1998), 2 cm of sediment represents approximately four years of sedimentation. Close to tidewater glaciers, sediment accumulation rates increase to more than 10 cm y^{-1} (Filipowicz, 1990), resulting in a shorter time represented by the sampled sediment. However, our stations are located mainly in the middle and outer parts of the fjords, along their main axes (Figure 1). Therefore, we assume that 2 cm of sampled sediment should, on average, represent approximately two years of sedimentation. Although this approach might seem to be an oversimplification since the time interval represented by the 2 cm thick sample differs at each station, we consider it reasonable for the aim of the study as we assume that the environmental conditions did not change drastically over the last couple of years. After thawing, 3–4 cm^3 of well-mixed sediment was placed in a polypropylene test tube, dried at >40°C and weighed with an analytical balance. The samples were subsequently soaked with distilled water for 12 h, centrifuged at 3600 rpm for 6 min and then processed using a standard palynological technique (e.g., Pospelova et al., 2010, 2005).

Marker grains of a known number of *Lycopodium clavatum* spores (e.g., Mertens et al., 2012a, 2009) were added to allow quantitative estimates of the absolute concentrations of dinocysts. About 7 ml of hydrochloric acid (HCl, 10%) at room temperature was slowly added to samples to dissolve the *L. clavatum* spore tablets and remove carbonates. After 30 minutes samples were centrifuged and decanted. Subsequently, ∼9 ml of distilled water was added and samples were centrifuged and decanted again. The procedure was repeated until the pH of the supernatant reached a neutral level. Afterwards, the samples were wet-sieved through 125 μm and 15 μm mesh to remove fractions of sediment above and below the maximal and minimal size of dinocysts.

After sieving, centrifuging, and decanting, ∼7 ml of room-temperature hydrofluoric acid (HF, 48%) was added to the sediment to remove silicate. Samples were left in a fume hood for 72 hours, with regular digestion checking and stirring. After silicate dissolution, samples were once again centrifuged and decanted and ∼7 ml of hydrochloric acid (HCl, 10%, at room temperature) was added. Samples were rinsed with distilled water as described above and sieved through a 15 μm mesh. Aliquots of a few drops of sample residue were placed on a glass slide and left for 24 h at room temperature to dry. Glycerine gel was used to mount a cover slide to the glass slide.

Approximately 300 specimens (min 281, max 319) were counted from each sample. Dinocysts were identified to the lowest possible taxonomical level. The paleontological taxonomy system used throughout this paper follows Zonneveld (1997), Kunz-Pirrung (1998), Montresor et al. (1999), Rochon et al. (1999), Head et al. (2001), Pospelova and Head (2002), Moestrup et al. (2009), Mertens et al. (2015, 2013, 2012b), and Zonneveld and Pospelova (2015). Cysts with unknown taxonomic affinity were classified into one of four groups: unidentified 1 – round transparent cyst, unidentified 2 – spiny transparent cyst, RBC – round brown cyst and SBC – spiny brown cyst. Cysts of *Biecheleria* cf. *baltica* are mostly very small (∼5–10 μm) and were partly lost during sample preparation (sieving). Therefore, we excluded them from the total cyst concentrations and statistical analyses. Furthermore, it cannot be excluded that some thin-walled transparent *Impagidinium* spp. cysts have been missed during the counting.

3.3. Benthic foraminifera sample preparation and faunal analysis

Living benthic foraminifera can be found down to 10 cm in sediment (e.g., Kucharska et al., 2019; Zajączkowski et al., 2010). However, as the gravity corer did not penetrate deep enough at every station, the uppermost 4 cm of sediment was used for foraminiferal analysis to enable the comparison of the results between all the stations. Even though the 4 cm thick samples might contain some foraminiferal specimens older than ∼2 years (as assumed for the 2 cm thick samples used for dinoflagellate cyst assemblage analysis), we find this a reasonable approach because, as mentioned before, we expect the environmental conditions to be roughly similar over the last couple of years. The sediments were weighed and wet-sieved through sieves with mesh sizes of 500 μm, 100 μm, and 63 μm. The 500 μm sieve was used only to protect foraminiferal shells from crushing by larger grains and the results of the analysis of >500 μm and 500–100 μm fractions (>100 μm) were analyzed together. The material was subsequently dried and weighed with an accuracy of ±0.1 mg. Benthic foraminifera census counts were conducted on representative splits (>300 specimens) in the >100 μm fraction using a Nikon SMZ1500 stereomicroscope. Individual species were identified and counted. The paleontological taxonomy system used throughout this paper follows Loeblich and Tappan (1987), Hald and Korsun (1997), Husum and Hald (2004), Darling et al. (2016), Łącka and Zajączkowski (2016), and Hayward et al. (2020). The number of benthic foraminifera per 1 g dry sediment (foram g^{-1}) was calculated.

3.4. Environmental data

The SST and SSS data were retrieved from the Copernicus website (https://www.copernicus.eu/; accessed October and November 2018). Monthly averaged data were read from available maps and average seasonal values were calculated over the period of two years prior to sediment sampling (August 2012–August 2014 for Hornsund and Storfjorden, August 2014–August 2016 for the rest of the stations; see Table 1 for sampling dates). Data on sea-ice coverage were retrieved from the website of the Norwegian Meteorological Institute (https://cryo.met.no/). Sea-ice concentrations at each station (in %) were manually read from Ice Charts at weekly intervals (four daily values per month) within two years prior to sediment sampling (the same as for the SST and SSS data). Subsequently, the average seasonal values (winter: December–February, spring: March–May, summer: June–August, autumn: September–November) were calculated. As fast ice was not present at any station during the studied time, only drift ice is included in the analysis. Despite ongoing global changes, we assume that environmental parameters over two years represent average 'modern' conditions and display general trends over the last couple of years. For this reason, we analysed the re-

lationships between environmental parameters over a constant time interval (two years prior to sediment sampling) and the two groups of microorganisms, despite the variable time represented by the sediment samples studied.

3.5. Statistical analyses

To reduce noise in the data sets, all statistical analyses were performed on relative abundances of dinocysts and benthic foraminifera after grouping some less important species into genera and excluding taxa that contribute less than 1% to the assemblages (i.e., the maximum relative abundance at any station was lower than 1%). Only these taxa are presented and discussed hereafter. Multivariate statistical analyses were used to investigate the relationships between each microfossil group (dinocysts and benthic foraminifera) and environmental parameters using CANOCO 4.5 for Windows (ter Braak and Šmilauer, 2002). First, a Detrended Correspondence Analysis (DCA) was performed to identify the nature of variability within the assemblages in each group. The length of the first gradient determines whether the assemblages have unimodal variation (length >2) or linear variation (length <2) (Lepš and Šmilauer, 2003). We identified that the length of the first gradient was 1.9 standard deviations (SD) for dinocysts and 2.4 SD for foraminifera, indicating a linear variation for cysts and a unimodal variation for foraminifera. The DCA results justified the further use of a Redundancy Analysis (RDA) for dinocysts and Canonical Correspondence Analysis (CCA) for benthic foraminifera (Lepš and Šmilauer, 2003).

We applied a forward selection of environmental parameters to reduce the set of variables that could effectively explain the greatest amount of variance in the data sets. A total of seven environmental parameters were chosen for the analyses: water depth (WD), winter and summer sea-surface temperature (SST win, SST sum), salinity (SSS win, SSS sum), and sea ice cover (SI win, SI summer). Each environmental variable's statistical significance (P-value < 0.05) was determined using the forward selection Monte Carlo permutation test, with 499 unrestricted permutations.

4. Results

4.1. Oceanographic conditions

The results of CTD measurements, together with the identified water masses (following Cottier et al., 2005) are shown in Figure 2. Seasonally averaged sea-ice cover, SST and SSS data used for the multivariate statistical analysis are listed in Supplementary Table 1. We acknowledge that some of the salinity data retrieved from Copernicus appear anomalous, reaching up to 37.8 at station WIJ1 in March. Such high values might be caused by the quality of satellite measurements in inner parts of narrow fjords and/or in high latitudes in general. However, it should be noted that the highest salinities (>35.3) are associated with the lowest temperatures (≤ -2°C), generally high sea-ice concentrations, and occur in the inner parts of the north-facing fjords (Wijdefjorden and Rijpfjorden) in winter and spring (January to May). Altogether, it suggests that the high salinities might be related to brines formed by salt rejection during sea-ice formation (Haarpaintner et al., 2001). For this reason, we decided not to discard or correct the outlying data as they most probably reflect the natural variations even if the absolute values are indeed overestimated.

4.2. Dinoflagellate cyst abundances and assemblages

The total cysts concentrations calculated per gram of dry weight of sediments (cysts g^{-1}) vary from ~1,700 to 20,000, with an average of ~10,800 cysts g^{-1}. The highest cyst concentrations were found in Isfjorden and Rijpfjorden. The southern part of the studied region is characterized by lower cyst concentrations, with the lowest values recorded at the Hornsund and Edgeøya sites (Figure 3A). In total, dinocysts belonging to 39 taxa (23 genera) were identified in the analysed samples. A total of 19 of them were produced by autotrophic and 20 by heterotrophic dinoflagellates (Supplementary Table 2). The proportions of cysts produced by heterotrophic and autotrophic dinoflagellates in the assemblages are variable. Figure 3B shows the geographical distribution of the heterotrophic/autotrophic-related taxa in the cyst assemblages. The proportion of heterotrophic taxa ranges from 21 to 81%, averaging ~53%. In general, the highest abundances of heterotrophic taxa were observed at the sites near the mouth of each fjord and in coastal waters, with the highest average values recorded in Isfjorden. *Islandinium minutum*, *Brigantedinium* spp., cysts of *Pentapharsodinium dalei* and *Polarella glacialis* were present in every sample (Figure 4). Six further taxa (*Ataxiodinium* spp., cysts of *Protoceratium reticulatum* (or *Operculodinium centrocarpum* sensu Wall and Dale, 1966), *Nematosphaeropsis labyrinthus*, *Dubridinium* spp. *Echinidinium* spp., and *Selenopemphix quanta*) were present in each of the studied regions (though not in every sample). Light microscope micrographs of the most common dinocyst taxa are shown in Figure 5.

Four species were most abundant in the analyzed samples (Figure 4). *Islandinium minutum* constituted ~39% of all identified dinocysts and reached a maximum of 72% at station IS 3. The second most abundant species were cysts of *Polarella glacialis* (~24%) with a maximum abundance of 73% at station NAL 1. Cysts of *Pentapharsodinium dalei* and *Operculodinium centrocarpum* contributed an average of ~9% and ~7% in all identified assemblages, respectively with maximum abundances of ~39% at WIJ 1 and ~29% at IS 1, respectively. Among the remaining taxa, only *Islandinium*? *cezare* reached more than 22% at one of the stations (HR 2) but its average proportion among all identified taxa was only ~3%. Details on the relative abundances of individual taxa at each station can be found in Supplementary Table 2.

The results of the Redundancy Analysis (RDA) on the proportions of dinocyst taxa in the assemblages showed that the first ordination axis explains 43% of the variance, and it is positively but not significantly correlated with the winter sea-ice cover and negatively and significantly correlated with the water depth (Figure 6). A Monte Carlo permutation test under the reduced model with 499 permutations indicated that the first ordination axis and all canonical axes are

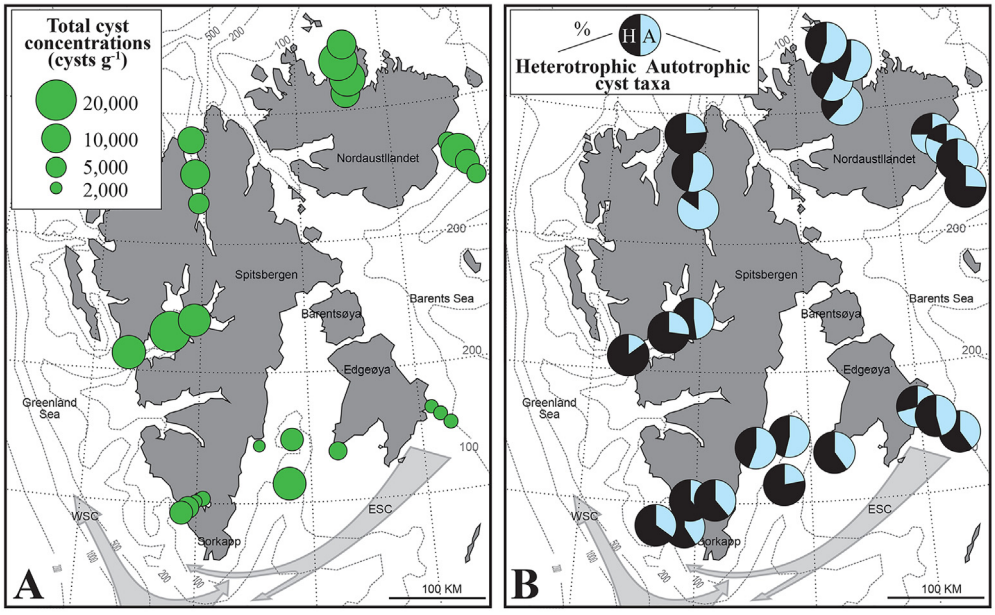

Figure 3 A: Total sedimentary concentrations [cysts g^{-1}] of dinocysts at each station. B: Proportion of autotrophic/heterotrophic dinocysts in each sample.

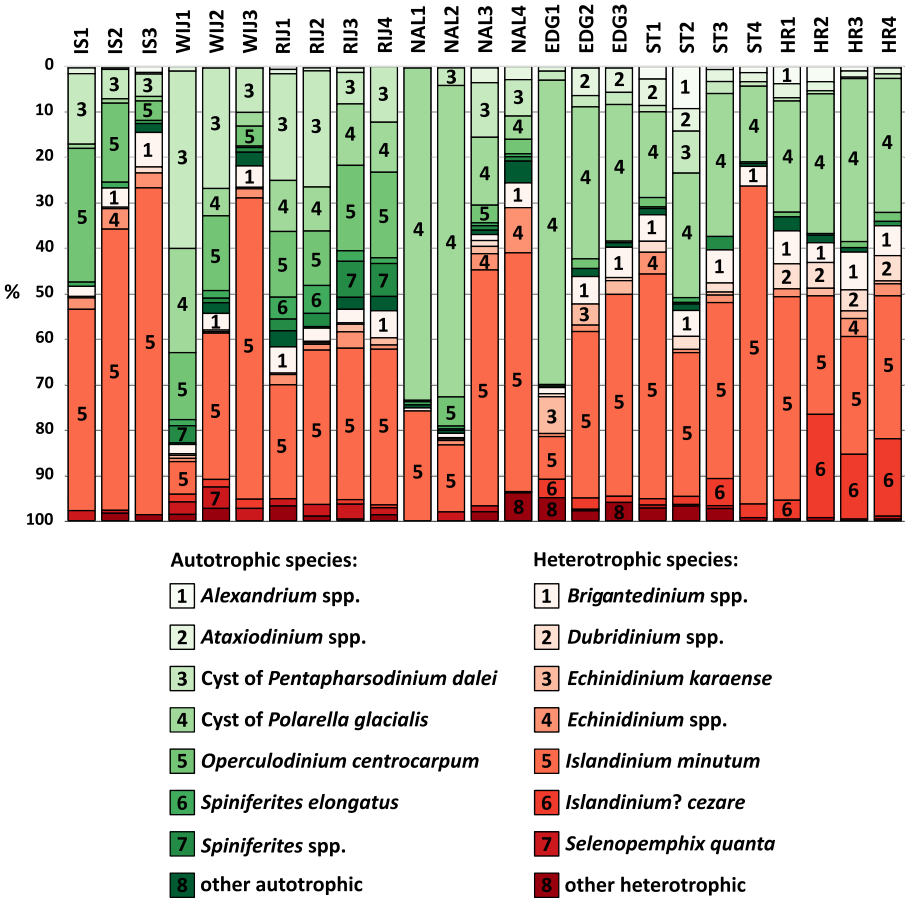

Figure 4 Percentages of the most common autotrophic (shades of green) and heterotrophic (shades of red) dinocyst taxa at each station.

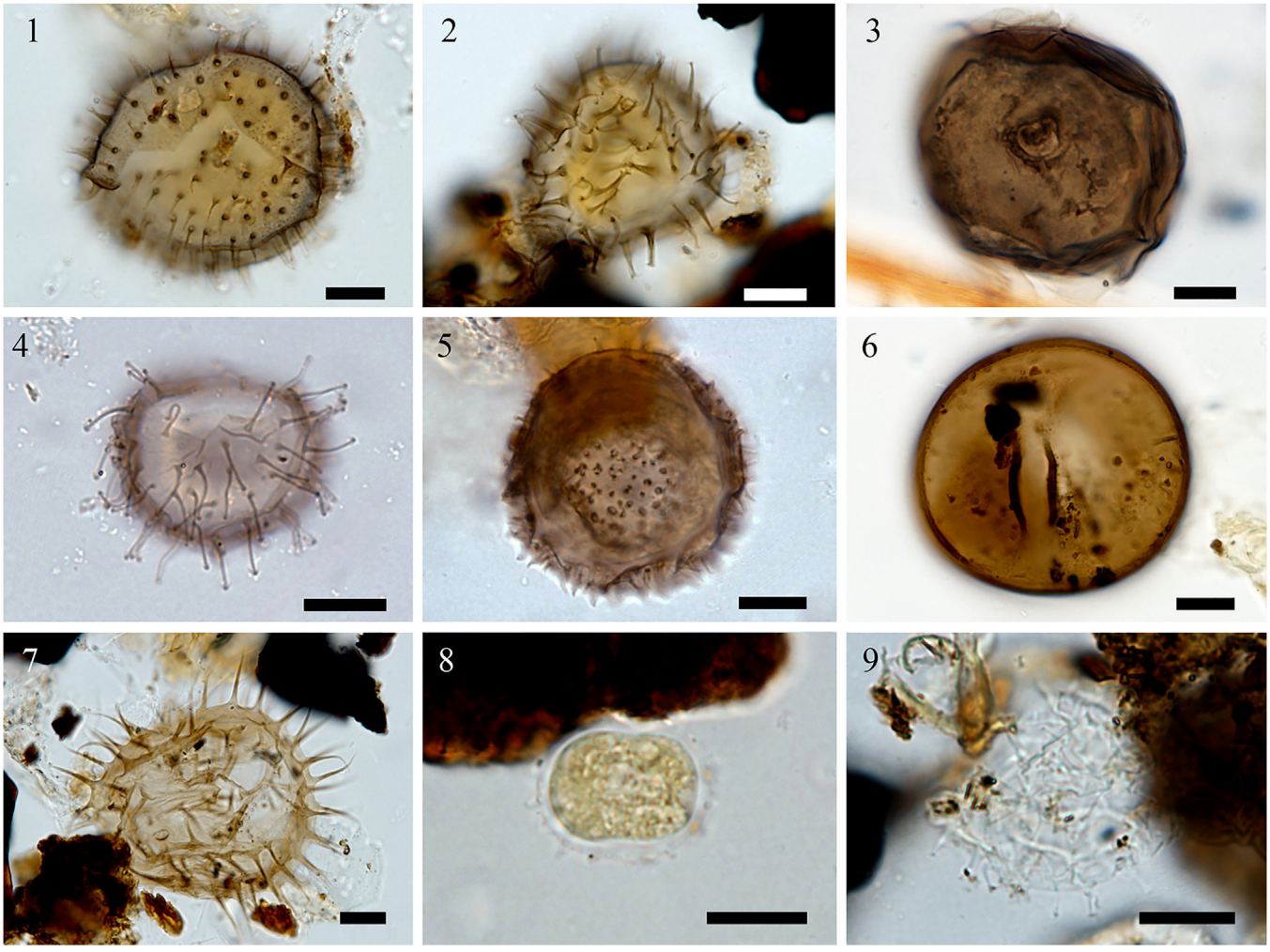

Figure 5 Plate presents light microscope micrographs. 1) High focus of *Islandinium minutum* (EDG 1). 2) High focus of *Echinidinium karaense* (EDG 1). 3) Mid focus of *Dubridinium* sp. with flagellar scar (HR 3). 4) High focus of *Islandinium*? *cezare* (EDG 1). 5) Mid focus of *Echinidinium sleipnerensis* (EDG 1). 6) Mid focus of *Brigantedinium simplex* with typical flagellar scars (NAL 4). 7) High focus of *Selenopemphix quanta* (EDG 1). 8) Mid focus of cyst of *Polarella glacialis* (EDG 1). 9) High focus of cyst of *Pentapharsodinium dalei* (IS 1). All scale bars = 10 μm.

statistically significant with P-values of 0.004 and 0.002, respectively. The second ordination axis explains an additional 19% of the variance, and it is positively and significantly correlated to the summer sea-ice cover and sea-surface salinity in winter. Figure 6 shows the ordination of sites, winter and summer environmental parameters, as well as the most common cyst taxa based on the first two RDA axes (RDA1 and RDA2). The first axis (RDA 1) demonstrates that the best fit corresponds to cysts of *Polarella glacialis* (67%), *Islandinium minutum* (37%), *Operculodinium centrocarpum* (24%), and *Echinidinium* species (~20%). The species with the best fit for the second axis (RDA 2) are cysts of *Pentapharsodinium dalei* (78%), *Spiniferites elongatus* (43%), *Selenopemphix quanta* and cysts of *Protoperidinium nudum* (both ~30%, respectively), and *Operculodinium centrocarpum* (27%).

The scores of RDA 1 and RDA 2 for each site are plotted on the satellite image of the area (NASA; https://landsat.visibleearth.nasa.gov/view.php?id=86468) that shows snow/ice cover in the summer of 2015 (Figure 7). It illustrates the impact of the warm WSC on the western side and the cool ESC on the southern and eastern coasts of Svalbard during the summer growing season. The figure shows that sites with the highest negative RDA 1 scores are in Isfjorden, Wijdefjorden, and Rijpfjorden, while the highest positive RDA1 values are in Nordaustlandet and Edgeøya. Sites with positive RDA 2 scores are primarily in Wijfjorden and Rijpfjorden, whereas sites with the highest negative scores of RDA 2 are found along the eastern and southern sites, as well as near the mouths of most of the fjords.

4.3. Benthic foraminiferal abundances and assemblages

The total benthic foraminifera concentrations calculated per gram of dry weight of sediments (forams g^{-1}) vary from 5 to ~1,300, with an average of ~214 forams g^{-1}. The highest benthic foraminiferal concentrations were found at Wijdefjorden and Nordaustlandet sites. The southern part of the studied region is characterized by lower foraminiferal concentrations, with the lowest values recorded at Stor-

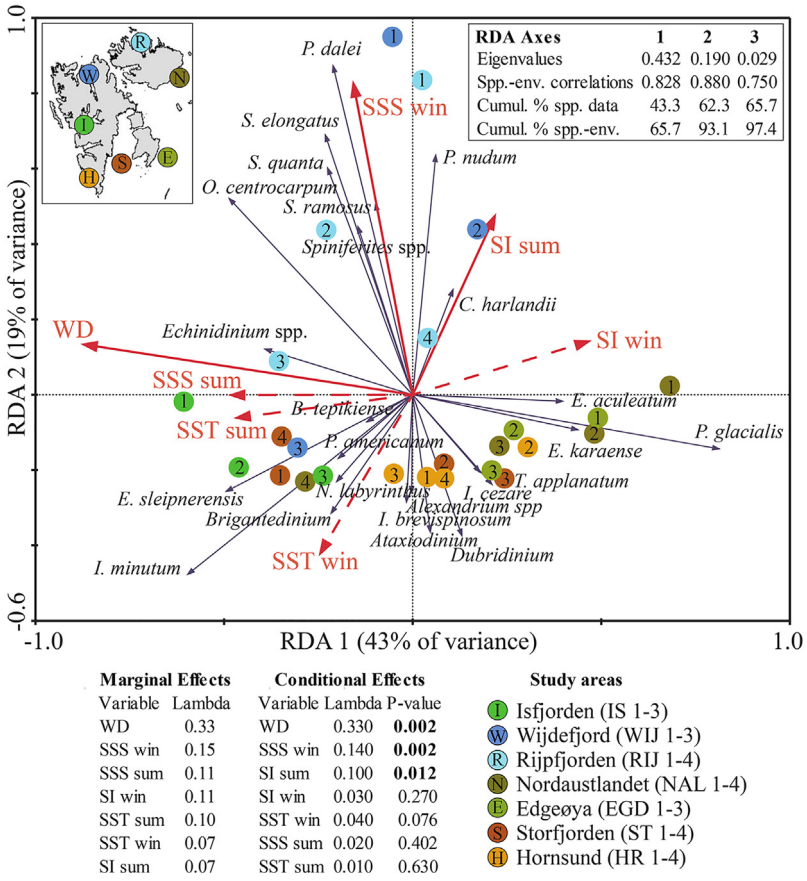

Figure 6 The results of the Redundancy Analysis (RDA) on the proportions of dinocyst taxa in the assemblages showing the ordination of sites, winter (win) and summer (sum) environmental parameters (SI — sea-ice concentration, SSS — sea surface salinity, SST — sea surface temperature), as well as the most common dinocyst taxa based on the first two RDA axes (RDA1 and RDA2).

fjorden and Edgeøya sites (Figure 8A). In total, benthic foraminifera belonging to 27 taxa (24 genera) were identified in the analysed samples. A total of 15 of them were calcareous and 12 were agglutinated (Supplementary Table 3). The proportions of calcareous and agglutinated foraminifera in the assemblages are variable. Figure 8B shows the geographical distribution of the calcareous/agglutinated taxa in the foraminiferal assemblages. The proportion of calcareous taxa ranges from 21 to 100%, averaging ~76%. In general, the highest proportions of calcareous taxa were observed at the sites near the fjord heads and stations closest to the coast, with the highest average values recorded in Wijdefjorden. *Elphidium clavatum*, *Islandiella helenae* and *Nonionellina labradorica* were present in every sample (Figure 9). Fourteen further taxa (*Buccella frigida*, *Cassidulina reniforme*, *Cibicides*, *lobatulus*, *Globobulimina arctica-turgida*, *Islandiella norcrossi*, *Stainforthia loeblichi*, *Trifarina fluens*, *Adercotryma glomeratum*, *Labrospira crassimargo*, *Recurvoides turbinatus*, *Reophax scorpiurus*, *Spiroplectammina* spp., *Textularia earlandi-kattegatensis*, and *Portatrochammina karica*) were present in each of the studied regions (though not in every sample).

Five benthic foraminifera species were dominant in most of the analyzed samples (Figure 9). *E. clavatum* constituted ~22% of all identified forams and reached a maximum of ~52% at station HR 2. The second most abundant species were *Cassidulina reniforme* and *Cibicides lobatulus* (15%, respectively) with a maximum abundance of ~71% at station HR 1 and ~48% at station WIJ 2, respectively. *Nonionellina labradorica* reached ~11% with a maximum abundance of ~31% at station IS 2. *Adercotryma glomeratum*, the most abundant agglutinated species, constituted ~8% of all identified taxa with a maximum of ~23% at station RIJ 1. Among the remaining species, *Melonis barleeanus* reached a maximum of ~12% at station NAL 3 but its average share among all identified taxa reached only ~2%. Details on the relative abundances of individual taxa at each station can be found in Supplementary Table 3.

The results of the canonical correspondence analysis (CCA) on the proportions of benthic foraminifera in the assemblages showed that the first ordination axis (CCA 1) explains 21% of the variance, and the second ordination axis (CCA 2) describes an additional 11% of the variance (Figure 10). The first and all canonical axes are statistically significant with P-values of 0.02 and 0.004, respectively. CCA 1 is positively and significantly correlated with the summer sea-ice cover, whereas CCA 2 is positively and significantly correlated with the winter sea-ice cover.

The first axis (CCA 1) has the best fit with agglutinated foraminifera *Adercotryma glomeratum* (55%), *Ammodiscus* sp. (58%), *Portatrochammina karica* (46%) and calcareous

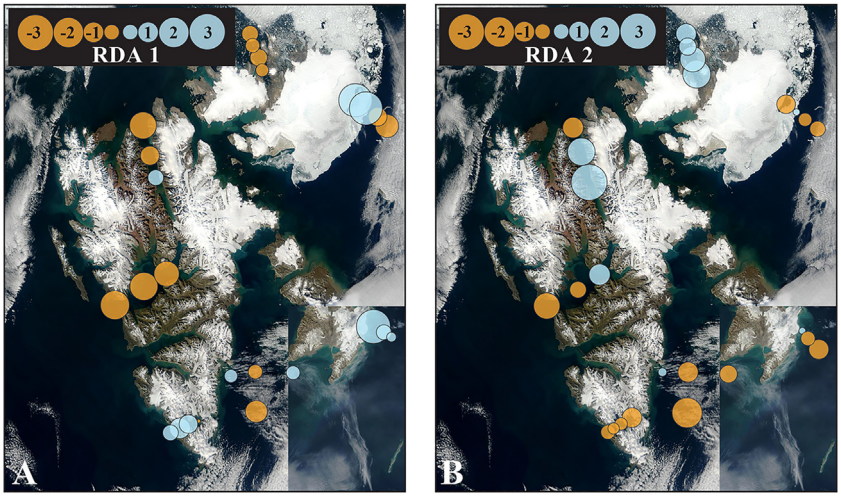

Figure 7 The scores of RDA 1 and RDA 2 for each site plotted on the satellite image of the area (NASA; https://landsat.visibleearth.nasa.gov/view.php?id=86468) showing snow/ice cover in the summer of 2015 (Data date: April 29, 2015—July 9, 2015).

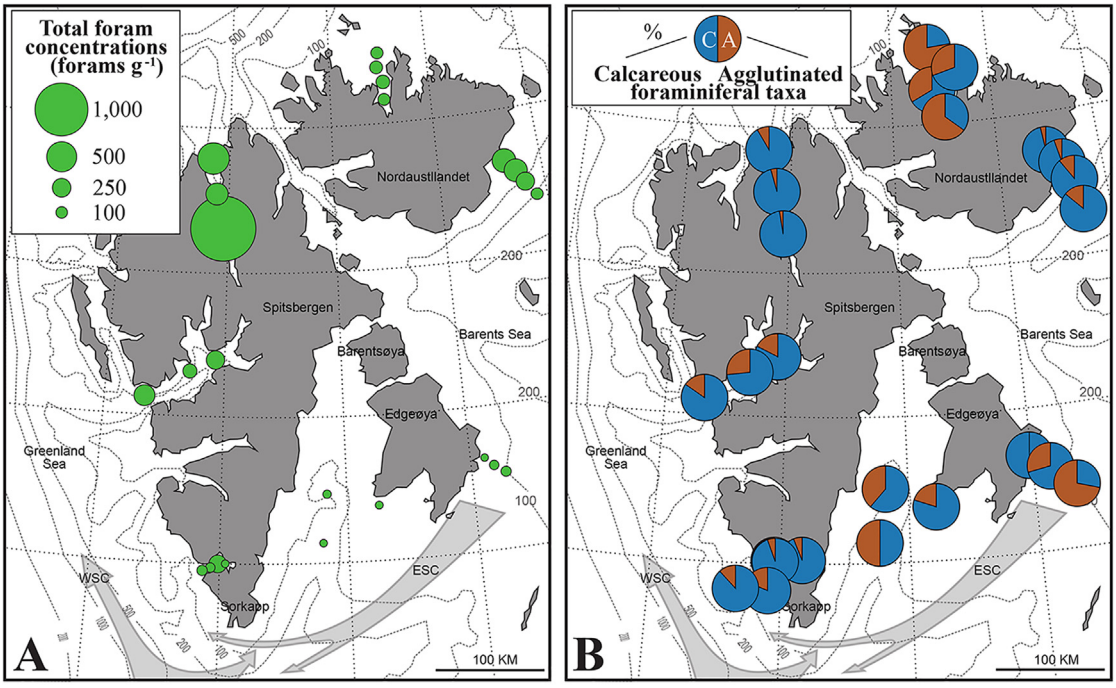

Figure 8 A: Total sedimentary concentrations [forams g^{-1}] of benthic foraminifera at each station. B: Proportion of calcareous/agglutinated foraminifera in each sample.

Melonis barleeanus (57%) and *Quinqueloculina* spp. (31%). The taxa with the best fit for the second axis (CCA 2) are calcareous *Cibicides lobatulus* (42%) and *Nonionellina labradorica* (28%). The CCA scores for each site plotted on the satellite image of the area (NASA; https://landsat.visibleearth.nasa.gov/view.php?id=86468) (Figure 11) show that the highest positive CCA 1 values are in Rijpfjorden and the highest negative values at the coastal sites of Nordaustlandet (NAL 1 and 2). Sites with positive CCA 2 scores are mainly in the northern and northeastern parts of the archipelago, whereas sites with the highest negative scores of CCA 2 are along the eastern and southern sites, as well as near the mouths of most of the fjords.

As mentioned above, the stations can be divided into three major areas. This classification has been confirmed by our dinocyst and benthic foraminiferal results and can be summarized as follows:

4.4. Atlantic Water-dominated stations

This region includes three westward and northward facing fjords: Isfjorden, Wijfjorden, and Rijpfjorden (Figure 1). These fjords are characterized by the presence of a thick layer of AW, usually underlain by TAW and covered by a relatively thin layer of SW and/or IW (Figure 2A). The dinocyst assemblages (Figure 4) are dominated by *Islandinium min-*

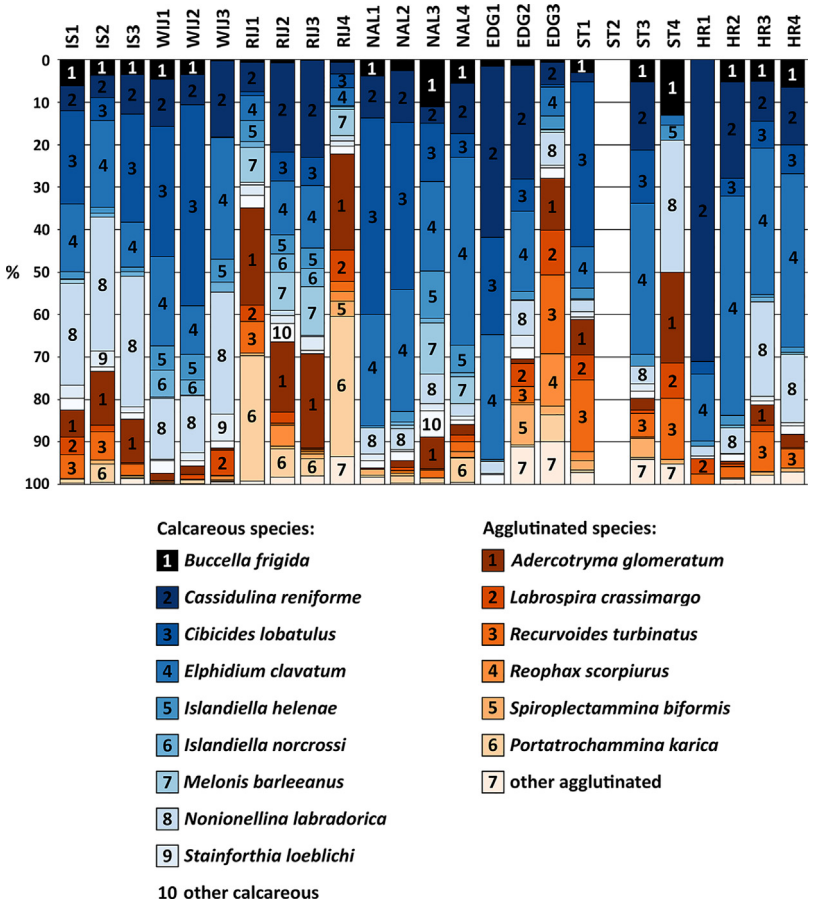

Figure 9 Percentages of the most common calcareous (shades of blue) and agglutinated (shades of brown) benthic foraminiferal species.

utum (an average abundance of ~41% with a maximum of 72% at station IS 3), followed by cysts of *Pentapharsodinium dalei* (~17% with a maximum of 37% at station WIJ 1), *Operculodinium centrocarpum* (~14% with a maximum of 28% at station IS 1), and cysts of *Polarella glacialis* (~8%). The most common benthic foraminiferal species (Figure 9) of the AW-dominated region are *Cibicides lobatulus*, *Nonionellina labradorica*, and *E. clavatum* (each constituting on average 15% of the assemblages), followed by *Adercotryma glomeratum* (~12%), *Cassidulina reniforme* (~11%), and *Portatrochammina karica* (~8%). *Cibicides lobatulus* reached a maximum abundance of 47% at station WIJ 2, *Nonionellina labradorica* reached 31% at station IS 2, and *Adercotryma glomeratum* reached 23% at station RIJ 1. Other dinocyst and benthic foraminiferal species constituted on average less than 5% of the assemblages, respectively.

4.5. Arctic Water-dominated stations

Fjords characterized by ArW dominance include Storfjorden and Hornsund, both located in southern Svalbard (Figure 1). Even though AW and TAW are also present in the water column at most of the stations, the overlying layer of SW and/or IW is relatively thicker, compared to AW-dominated stations, and the surface water temperatures are lower (Figure 2C). The most common dinocyst species in this region (Figure 4) include *Islandinium minutum* (~40%), cysts of *Polarella glacialis* (~27%), and *Islandinium? cezare* (~9% with a maximum of 22% at station HR 2). The most numerous benthic foraminiferal species (Figure 9) are *E. clavatum* (~27% with a maximum of 52% at station HR 2), *Cassidulina reniforme* (~19% with a maximum of 71% at station HR 1), *Nonionellina labradorica* (~12%), *Cibicides lobatulus* (~10%), *Recurvoides turbinatus* (~8%), *Adercotryma glomeratum* (~6%), and *Buccella frigida* (~5%).

4.6. Locally/glacier-influenced stations

This region groups stations located in the coastal zones of Nordaustlandet and Edgeøya (Figure 1). The oceanographic conditions and, thus, dinocyst and benthic foraminiferal faunas are the most diversified here and depend largely on the distance of the station from the ice front. SW, IW, and TAW dominate the water column in different proportions at all the stations, indicating a dynamic oceanographic regime and the mixing of water masses of different origins (Figure 2B). Two species dominate the dinocyst assemblages (Figure 4) in this region: cysts of *Polarella glacialis* (~41% with a maximum of 72% at station NAL 1) and *Islandinium minutum* (~33%). The most common benthic foraminiferal species (Figure 9) include *E. clavatum* (~25%), *Cibicides lobatulus* (~19%), *Cassidulina reniforme* (~16%), and *Non-*

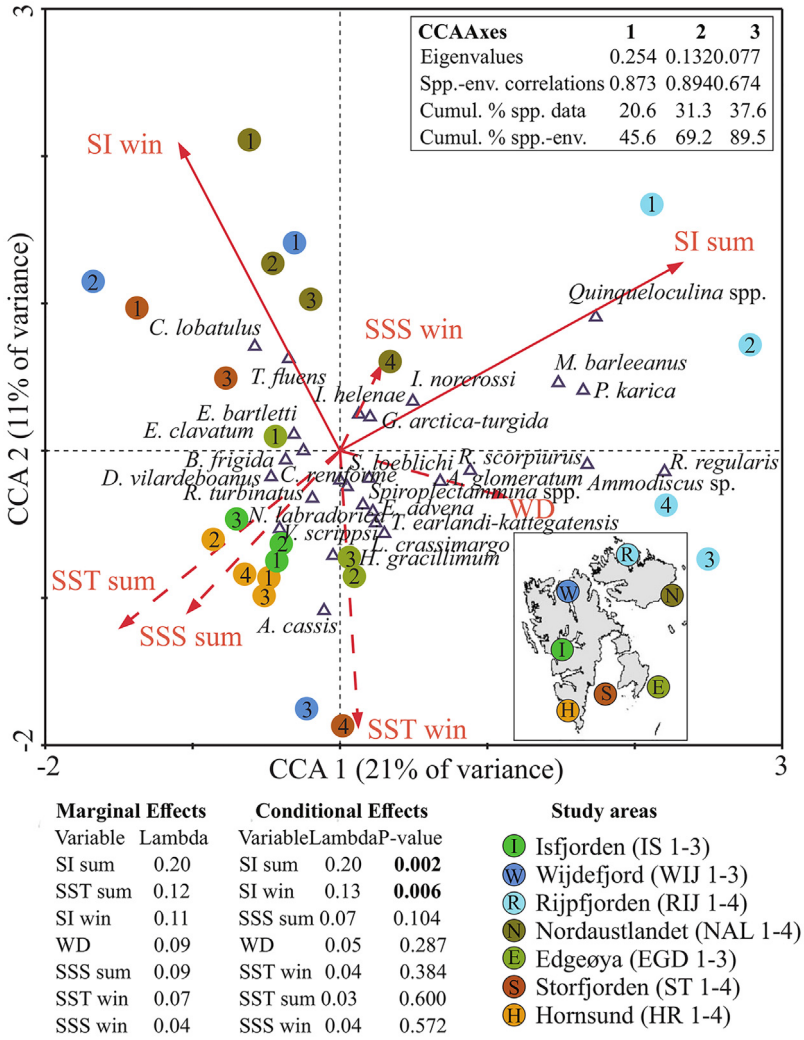

Marginal Effects

Variable	Lambda
SI sum	0.20
SST sum	0.12
SI win	0.11
WD	0.09
SSS sum	0.09
SST win	0.07
SSS win	0.04

Conditional Effects

Variable	Lambda	P-value
SI sum	0.20	**0.002**
SI win	0.13	**0.006**
SSS sum	0.07	0.104
WD	0.05	0.287
SST win	0.04	0.384
SST sum	0.03	0.600
SSS win	0.04	0.572

Study areas

- I Isfjorden (IS 1-3)
- W Wijdefjord (WIJ 1-3)
- R Rijpfjorden (RIJ 1-4)
- N Nordaustlandet (NAL 1-4)
- E Edgeøya (EGD 1-3)
- S Storfjorden (ST 1-4)
- H Hornsund (HR 1-4)

Figure 10 The results of the canonical correspondence analysis (CCA) on the proportions of benthic foraminifera in the assemblages showing the ordination of sites, winter (win) and summer (sum) environmental parameters (SI — sea-ice concentration, SSS — sea surface salinity, SST — sea surface temperature), as well as the most common benthic foraminiferal taxa based on the first two CCA axes (CCA1 and CCA2).

ionellina labradorica (~6%). It is also worth noting that *Melonis barleeanus* reached a maximum of 12% at station NAL 3 although its average share among all identified taxa reached less than 3%.

5. Discussion

Cyst-forming dinoflagellates and benthic foraminifera are two unrelated groups of microorganisms, but both encode environmental parameters of surrounding waters. Most dinoflagellates are planktic (e.g., Taylor et al., 2008; Zonneveld et al., 2013) and for this reason, their spatial distribution is mostly dependent on the upper water masses. In contrast, the composition of the benthic foraminiferal assemblages is strongly influenced by factors such as, e.g., trophic state, type of sediment, and bottom water oxygenation level that might be independent of the dominant water mass. As already mentioned in the introduction, we decided to focus only on surface water conditions, as these are available over extended periods of time from satellite observations, while bottom water parameters are available only from CTD measurements performed during research cruises, mostly in summer. Even though surface water parameters might not affect benthic foraminiferal assemblages in a straightforward way, in the relatively shallow (<300 m) waters around Svalbard they certainly influence them indirectly, e.g., by regulating the food flux reaching the bottom (see, e.g., Seidenkrantz, 2013). This difference is well reflected in our results. For instance, the first and second ordination axes of the RDA on the proportions of dinocyst taxa in the assemblages explain much more of the variance (43% and 19%, respectively, Figure 6) compared to the first two ordination axes of the CCA on the proportions of benthic foraminifera (21% and 11%, respectively, Figure 10).

The dinocyst concentrations (Figure 3A) clearly show that dinoflagellates are highly dependent on the properties of

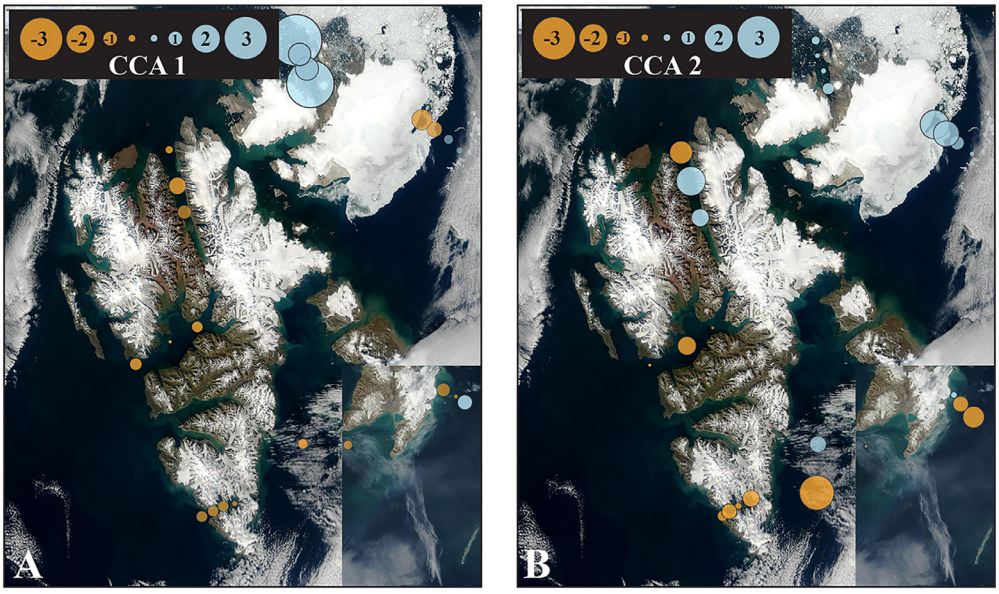

Figure 11 The scores of CCA 1 and CCA 2 for each site plotted on the satellite image of the area (NASA; https://landsat.visibleearth.nasa.gov/view.php?id=86468) showing snow/ice cover in the summer of 2015.

the upper water masses. The concentrations are highest in the western and northern Svalbard, most influenced by the WSC carrying AW. It might seem surprising that the dinocyst abundance is lower in Wijdefjorden than in the Rijpfjorden located farther north and more distant from the AW source. However, it should be noted that while Wijdefjorden is a long and narrow fjord, which limits AW penetration, Rijpfjorden has a wide mouth allowing for an easier exchange of water masses. Additionally, Rijpfjorden is strongly affected by summer sea ice (Figure 6) which might further promote summer dinoflagellate blooms as melting sea ice releases nutrients stimulating productivity in the marginal ice zone (e.g., Hebbeln and Wefer, 1991; Ramseier et al., 1999; Sakshaug, 2004; Smith Jr. et al., 1987). Off Nordaustlandet the dinocyst abundance is also relatively high (comparable to that in Wijdefjorden) indicating that AW reaches this area (Figure 2B). In southern Svalbard, the abundances are generally low. An exception is two stations in Storfjorden (ST 1 and 4) suggesting that the WSC can reach the main axis of this widely open fjord in times when the ESC weakens.

The benthic foraminiferal abundances exhibit a similar general pattern with higher values in western and northern areas influenced mainly by the WSC and lower values in the south affected by the ESC (Figure 8). A peculiar observation is that the highest benthic foraminiferal concentrations were found in Wijdefjorden (with by far the highest values at station WIJ 1 in the inner fjord) and Nordaustlandet. This might suggest that the benthic foraminiferal abundance is also stimulated by organic matter delivered by glaciers as both regions are influenced by tidewater ice fronts.

An important and widely debated aspect of dinocyst and benthic foraminifera distributions in coastal waters around Svalbard is their association with sea ice. Despite the recent development of geochemical proxies of sea-ice coverage (e.g., Belt et al., 2007; Belt and Müller, 2013; Cabedo-Sanz et al., 2013; Müller et al., 2011), its reconstruction in paleo records remains a complicated issue. For this reason, we took a particular interest in investigating the potential use of the two microfossil groups together as sea-ice indicators. More specifically, here we discuss drift ice as fast ice was not present at any station over the studied time.

An analysis of the dinocyst distribution around Svalbard suggests that two species might potentially be associated with sea ice: *Echinidinium karaense* and *Islandinium*? *cezare*. *Echinidinium karaense*, known from the Beaufort Sea, the Baffin Bay, and the northern Hudson Bay, prefers waters with temperatures between −2°C and −8°C and salinity between 20.5 and 33.8. It is found in nutrient-rich waters with lowered salinity due to ice melting and with a well-ventilated layer of bottom waters (e.g., Head et al., 2001; Zonneveld and Pospelova, 2015). Its association with sea ice has previously been investigated, but as it occurred only occasionally in areas with dense sea-ice cover, no definite conclusion have been reached (de Vernal et al., 2020, 2013). *Islandinium*? *cezare* is known from the Kara Sea and appears to have similar environmental preferences to *Echinidinium karaense* (e.g., Head et al., 2001; Zonneveld and Pospelova, 2015). The relative abundances of the two species were low at AW-dominated stations (Isfjorden, Wijdefjorden, Rijpfjorden) as well as off Nordaustlandet (Figure 3). They were much higher off Edgeøya and at ArW-dominated stations (Storfjorden and Hornsund). Nevertheless, they were present in all areas except for Isfjorden (Figure 12), i.e., in areas where sea ice occurs (Supplementary Table 1). Although our environmental data indicate very low sea-ice concentrations in Hornsund, its western and central part is often occupied by pack ice brought there from the Barents Sea by the ESC in late spring and summer (Błaszczyk et al., 2013). Altogether, this suggests that *Echinidinium karaense* and *Islandinium*? *cezare* could be potential regional sea-ice indicators.

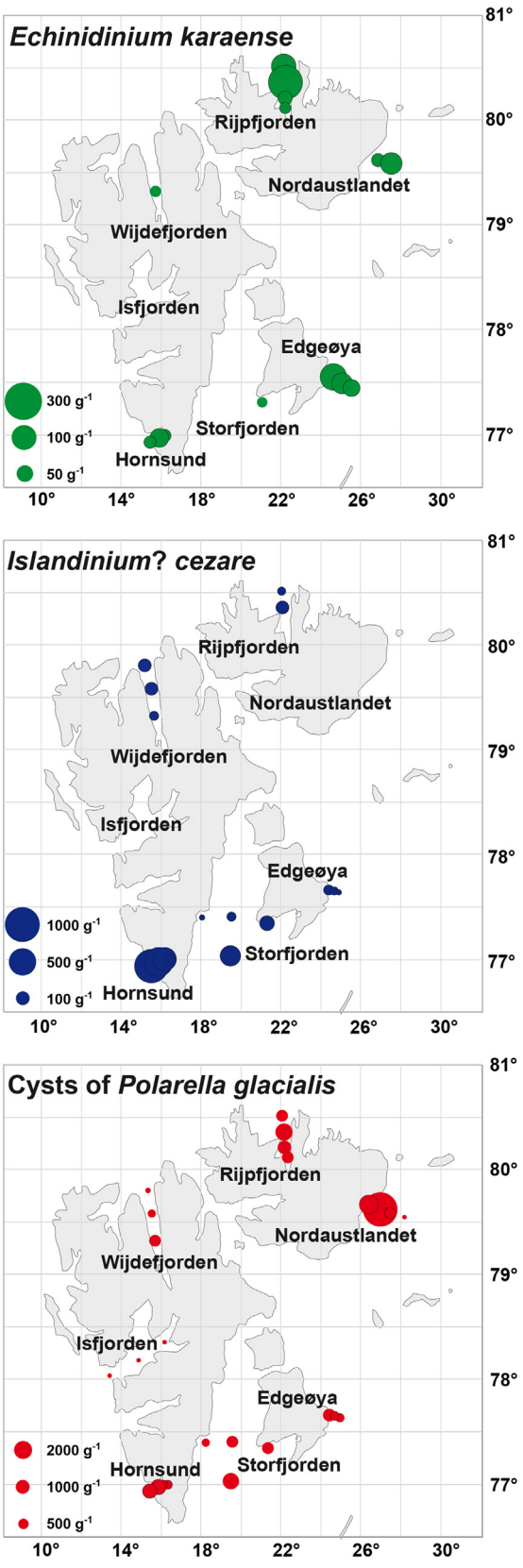

Figure 12 Sedimentary concentrations (cysts g^{-1}) of dinoflagellate cyst taxa potentially associated with sea ice: *Echinidinium karaense*, *Islandinium*? *cezare* and cysts of *Polarella glacialis*.

Our RDA results (Figure 6) show that the dinocyst species that is the most correlated with winter sea ice (drift ice) is *Polarella glacialis*. This species was first described from sea-ice brine channels in Antarctica (Montresor et al., 1999) and its association with sea ice has been observed in the Canadian Arctic (Montresor et al., 2003) and the Arctic Ocean (Matthiessen et al., 2005). However, cysts of *Polarella glacialis* have not been identified in most sediment samples used in paleoenvironmental studies for several potential reasons. Cysts of *Polarella glacialis* likely do not consist of resistant dinosporin (Montresor et al., 1999) and their long-term preservation in sediments is questionable. Furthermore, small (12—17-μm long and 8—15-μm wide) cysts of *Polarella glacialis* could easily pass through the 10—15 μm mesh size typically used in dinocyst sample preparation protocols, thus some but not all of them could be lost during palynological sample preparation (see Heikkilä et al., 2016, 2014). The abundance of this species in our samples (Figures 4 and 11) supports the fact that the cyst walls are resistant enough to be extracted from surface sediments and be used as environmental indicators, at least for modern samples from the Svalbard region. We acknowledge that some of the cysts of *Polarella glacialis* were partly lost during sample preparation. This may have biased our results, but the correlation of this species with sea-ice cover is still strong. *Echinidinium karaense* also shows a correlation with winter sea ice in the RDA plot (Figure 6). Even though it also appears in middle and outer Hornsund (stations HR 2-4) where no sea ice was recorded (Supplementary Table 1), the presence of *Echinidinium karaense* might be in accordance with episodic appearance of pack ice in this area in late spring and summer, as mentioned above. Thus, cysts of *Polarella glacialis* as well as *Echinidinium karaense* can be considered potential winter drift ice indicators in the Svalbard region. Nevertheless, it should be kept in mind that the first ordination axis of the RDA plot, which cysts of *Polarella glacialis* and *Echinidinium karaense* best fit with, is positively but not significantly correlated with the winter sea-ice cover.

No correlation was found between the winter sea-ice cover and the abundance of *Islandinium*? *cezare* (Figure 6). The discrepancy between the "naked eye" correlation of this species' distribution and sea-ice concentration and the RDA results might have several reasons. First of all, the environmental parameters had to be selected and reduced to enable an efficient statistical analysis. This might have led to some of the fauna-environment relationships being missed in the results. For instance, pack ice is brought from the Barents Sea into Hornsund mainly in late spring and summer (Błaszczyk et al., 2013), while our analysis took into account only winter and summer sea-ice concentrations. Secondly, the abundance of *Islandinium*? *cezare* was relatively low, compared to cysts of *Polarella glacialis* (though higher than that of *Echinidinium karaense*), which might have further biased the results. However, our results confirm previous findings (Heikkilä et al., 2016), indicating no direct relationship between *Islandinium*? *cezare* and sea-ice cover.

The CCA results of benthic foraminifera assemblages (Figure 10) show that the first ordination axis which is positively and significantly correlated with the summer sea-ice cover has the best fit mostly with agglutinated foraminifera species. However, before concluding that they can be used

as summer sea-ice indicators (e.g., Scott et al., 2008), it should be noted that agglutinated species are most abundant in outer parts of fjords and at sites located farther offshore (Figure 8B) and that the ratio of agglutinated to calcareous foraminifera mainly depends on the absolute abundance of the latter (Supplementary Table 3). Obviously, the summer sea ice that originates mostly from the Arctic Ocean and the Barents Sea is also the most abundant in the outer parts of the fjords. Therefore, our results do not provide a definite answer whether increased sea-ice concentration in summer is indeed an environmental preference of agglutinated species (or a factor that decreases the abundance of calcareous species) or are there other factors that determine lower abundances of calcareous foraminifera in the outer parts of fjords. Although benthic foraminifera are not direct proxies for sea-ice cover, they respond to the surplus of food often available at sea-ice edges (Hebbeln and Wefer, 1991; Seidenkrantz, 2013; Smith Jr. et al., 1987). Furthermore, poor preservation of calcareous tests results from intensive decay of organic matter, leading to a decrease in pH (Majewski and Zajączkowski, 2007), or corrosive brines released during sea-ice formation (Fossile et al., 2020; Nardelli et al., 2023), although the latter occurs mainly during the winter-early spring season.

Interesting exceptions among the calcareous fauna are *Quinqueloculina* spp. and *Melonis barleeanus*, both showing a strong correlation with the summer sea-ice cover (Figure 10). *Quinqueloculina* spp. is an epifaunal porcelaneous foraminifera that belongs to miliolids. In our samples, it consisted mainly of *Quinqueloculina arctica*, a species common in the Arctic Ocean (e.g., Barrientos et al., 2018). It was the most common in the inner Rijpfjorden, where the summer sea-ice concentration was also the highest. Together, it might suggest that *Quinqueloculina* spp. or, more precisely, *Quinqueloculina arctica*, can be used as an indicator of summer sea ice in this particular environmental setting (a fjord facing the Arctic Ocean). *Melonis barleeanus*, in turn, is an infaunal hyaline species that is usually associated with fine-grained sediments containing buried organic matter that supports an infaunal life habit (e.g., Hald and Steinsund, 1992; Jennings et al., 2004). The species was first recorded in Rijpfjorden only recently and its appearance in this fjord was associated with the increasing influence of AW on the northern coast of Svalbard (Kujawa et al., 2021). Although this might be true, we suppose that the relatively high abundance of this species in Rijpfjorden and off Nordaustlandet compared to other stations (Figure 9) results mainly from its known environmental preferences. However, locations with abundant summer sea ice might also be characterised by fine-grained sediments transported by the ice (e.g., Nürnberg et al., 1994), thus making *Melonis barleeanus* an indirect summer sea-ice indicator.

Winter sea ice is the most abundant in the inner parts of the fjords (especially Wijdefjorden and Storfjorden) and off the glaciated shores (Supplementary Table 1). These also happen to be the areas where the relative abundance of calcareous forams is the highest, which is most clearly seen at stations off Edgeøya (Figure 8B). As a result, CCA shows a correlation between winter sea-ice concentration and several species of calcareous benthic foraminifera (Figure 10). However, this does not mean that they can be simply interpreted as winter sea-ice indicators. A good example is *Cibicides lobatulus*, the species the most correlated with winter sea-ice cover according to our CCA results. It dominates at locations with coarse sediments and is usually interpreted as an indicator of high energy/low sedimentation rate environments (e.g., Klitgaard-Kristensen and Sejrup, 1996) in marine environments from the Arctic (e.g., Hald and Korsun, 1997) to the tropics (e.g., Javaux and Scott, 2003; Romano et al., 2022). In Svalbard, such conditions may occur in the vicinity of fjord thresholds and narrows, where sea ice produced in the inner parts may also get stuck for extended periods of time. The species was also common at stations close to the ice fronts of Nordaustlandet and Edgeøya (Supplementary Table 3) where the environment is extremely dynamic. Winter sea ice is also abundant near the ice fronts because of large amounts of freshwater from the glaciers, which freezes at higher temperatures than saline water. Taken together, this could have contributed to the correlation of *Cibicides lobatulus* with winter sea-ice cover in our statistical analysis. However, this correlation occurs only in the particular environmental setting of the Svalbard fjords and glaciated margins.

In contrast, *Nonionellina labradorica* occupies the outer, deeper parts of the western and southern fjords, influenced by stable TAW (Figure 2, Supplementary Table 3) as it is known to feed on fresh phytodetritus and thus is indicative of high-productivity environments (e.g., Hald and Korsun, 1997; Majewski et al., 2009; Polyak and Mikhailov, 1996; Zajączkowski et al., 2010). Therefore, its strong negative correlation with winter and summer sea-ice cover is not surprising.

A direct relationship between net primary production and the abundance of heterotrophic dinoflagellate species can be expected. This relationship is more complex for autotrophic species, as they produce part of the chlorophyll-*a* (Chl-*a*) registered by the satellites. When Chl-*a* concentrations increase, heterotrophic species generally increase more than autotrophic species, so that the latter decrease in relative abundance (e.g., Zonneveld et al., 2013). A positive correlation between Chl-*a* concentrations and benthic foraminiferal abundance in shallow shelf areas can also be expected (e.g., Ahrens et al., 1997; Yamashita et al., 2020). However, no such relationship can be observed in our data (Figures 3, 7 and 12). First, average sea surface Chl-*a* concentrations around Svalbard are generally low, except for a few areas like Freemansundet (north of Edgeøya), Van Mijenfjorden (on the western coast of Svalbard), or in some of the side-fjords of the Isfjorden system where they reach relatively high values of up to ~68 mg Chl yr^{-1} m^{-3} (Figure 13). Unfortunately, none of our stations is located in these net primary production hotspots and the highest, though moderate Chl-*a* concentrations can be found at Storfjorden stations ST 2 and ST 3. Second, in such complex environments as Arctic fjords (e.g., Cottier et al., 2005; Kujawa et al., 2021; Syvitski and Shaw, 1995) the relationship between the net primary production and the Chl-*a* concentration (e.g., Campbell et al., 2002) might be more complex and/or suppressed by other processes than in the open ocean. Potential factors that might influence the primary productivity in Arctic fjords include, e.g., increased turbidity of the water or enhanced sedimentation of organic matter at glacier fronts during the melting season (e.g., Kujawa et al., 2021; Svendsen et al., 2002).

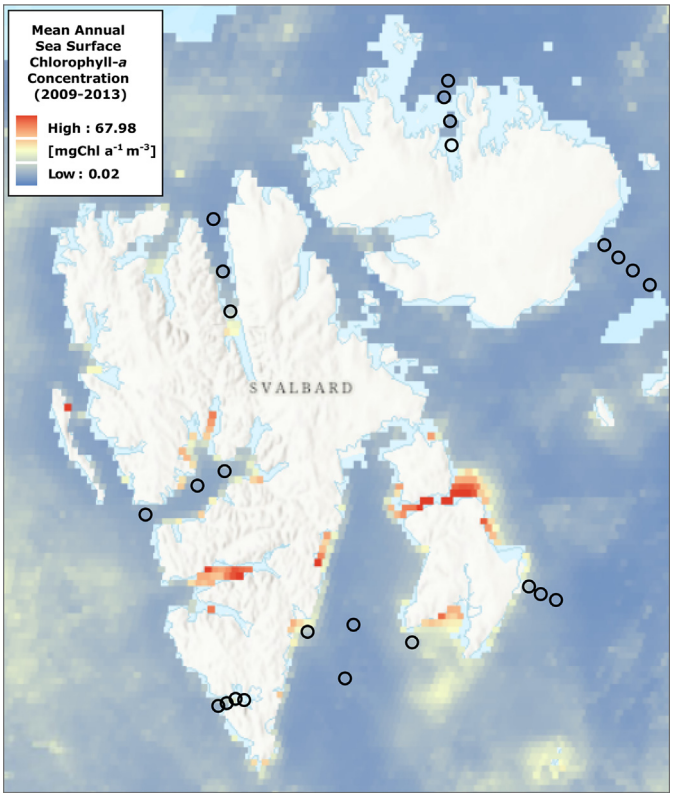

Figure 13 Location of study sites plotted on mean annual sea surface chlorophyll-*a* concentration [mgChl a^{-1} m^{-3}] data from satellite measurements (2009—2013). Data source: NASA Ocean Biology (OB.DAAC, 2014). Mean annual sea surface chlorophyll-*a* concentration for the period 2009—2013 (composite dataset created by UNEPWCMC). Data obtained from the Moderate Resolution Imaging Spectroradiometer (MODIS) Aqua Ocean Colour website (NASA OB.DAAC, Greenbelt, MD, USA). Accessed 28/11/2014. URL: http://oceancolor.gsfc.nasa.gov/cgi/l3. Cambridge (UK): UNEP World Conservation Monitoring Centre. URL: http://data.unep-wcmc.org/datasets/37.

6. Summary and conclusions

The fjords and glaciated coasts of the Svalbard archipelago are complex environments shaped by numerous factors. The most important of them is the AW-carrying WSC which mostly impacts the western coast, but its influence reaches as far as the coast of Nordaustlandet. It carries large amounts of heat, salt, and nutrients which have a tremendous effect on marine ecosystems, glaciers, and coasts. The abundance of both dinocysts and benthic foraminifera is clearly dependent on the strength of AW inflow. However, other factors such as the sea ice exported from the Arctic Ocean and the Barents Sea or even the shape and bathymetry of individual fjords strongly influence the planktic and benthic communities in the region.

The results of multivariate statistical analyses of the relationships between environmental parameters and dinocyst assemblages suggest that cysts of *Polarella glacialis* and *Echinidinium karaense* can be considered winter drift ice indicators. The potential association between *Islandinium*? *cezare* and sea-ice cover was not confirmed.

The relationships between environmental parameters and benthic foraminiferal assemblages are much more difficult to interpret, as the surface water parameters analysed in this study have only indirect influence on them. Furthermore, these bottom dwellers might be influenced by much more factors than just the dominant water mass or sea-ice cover. Although the statistical analysis shows the correlation of some benthic foraminiferal species or groups with winter/summer sea-ice cover, this correlation could be caused by more indirect relationships. For example, the correlation of *Melonis barleeanus* with summer sea-ice cover could be caused by the association of this species with fine-grained sediments, which around Svalbard are more common in areas with abundant summer sea ice.

In general, the analysis of relationships between the environmental parameters and the abundance of dinocyst and benthic foraminiferal species is a complicated task as even a strong correlation does not necessarily mean a causal relationship in such a complex environment as Svalbard fjords. Nevertheless, using two complimentary microfossil groups as (paleo)environmental indicators can provide a more complete picture of the environmental conditions.

Acknowledgements

Study design and data collection (dinocyst analyses) have been supported by grant no. 2014/15/N/ST10/05115 funded by the National Science Centre, Poland. Data collection

(foraminiferal analyses) and statistical analysis have been funded by Norwegian Financial Mechanism for 2014-2021, project no. 2019/34/H/ST10/00682. Data interpretation and manuscript preparation have been supported by grant no. 2020/39/B/ST10/01698 funded by the National Science Centre, Poland.

Declaration of competing interest

The authors declare that they have no competing interest.

Supplementary materials

Supplementary material associated with this article can be found, in the online version, at https://doi.org/10.1016/j.oceano.2023.06.007.

References

Aagaard, K., Foldvik, A., Hillman, S.R., 1987. The West Spitsbergen Current: Disposition and Water Mass Transformation. J. Geophys. Res. 92, 3778—3784.

Ahrens, M.J., Graf, G., Altenbach, A.V., 1997. Spatial and temporal distribution patterns of benthic foraminifera in the Northeast Water Polynya. Greenland. J. Marine Syst. 10, 445—465. https://doi.org/10.1016/S0924-7963(96)00052-8

Akimova, A., Schauer, U., Danilov, S., Núñez-Riboni, I., 2011. The role of the deep mixing in the Storfjorden shelf water plume. Deep-Sea Res. Pt. I 58, 403—414. https://doi.org/10.1016/j.dsr.2011.02.001

Ambrose, W.G., Caroll, M.L., Greenacre, M., Thorrold, S.R., McMahon, K.W., 2006. Variation in Serripes groenlandicus (Bivalvia) growth in a Norwegian high-Arctic fjord: Evidence for local- and large-scale climatic forcing. Glob. Change Biol. 12, 1595—1607. https://doi.org/10.1111/j.1365-2486.2006.01181.x

Balazy, P., Kuklinski, P., 2019. Year-to-year variability of epifaunal assemblages on a mobile hard substrate—Case study from high latitudes. Mar. Ecol. 1—17. https://doi.org/10.1111/maec.12533

Bamber, J.L., Krabill, W., Raper, V., Dowdeswell, J.A., 2004. Anomalous recent growth of part of a large Arctic ice cap: Austfonna, Svalbard. Geophys. Res. Lett. 31, 3—6. https://doi.org/10.1029/2004GL019667

Barbieri, R., Hohenegger, J., Pugliese, N., 2006. Foraminifera and environmental micropaleontology. Mar. Micropaleontol. 61, 1—3. https://doi.org/10.1016/j.marmicro.2006.06.004

Barrientos, N., Lear, C.H., Jakobsson, M., Stranne, C., O'Regan, M., Cronin, T.M., Gukov, A.Y., Coxall, H.K., 2018. Arctic Ocean benthic foraminifera Mg/Ca ratios and global Mg/Ca-temperature calibrations: New constraints at low temperatures. Geochim. Cosmochim. Acta 236, 240—259. https://doi.org/10.1016/j.gca.2018.02.036

Belt, S.T., Massé, G., Rowland, S.J., Poulin, M., Michel, C., LeBlanc, B., 2007. A novel chemical fossil of palaeo sea ice: IP25. Org. Geochem. 38, 16—27. https://doi.org/10.1016/j.orggeochem.2006.09.013

Belt, S.T., Müller, J., 2013. The Arctic sea ice biomarker IP 25: a review of current understanding, recommendations for future research and applications in palaeo sea ice reconstructions. Quaternary Sci. Rev. 79, 9—25. https://doi.org/10.1016/j.quascirev.2012.12.001

Błaszczyk, M., Jania, J.A., Kolondra, L., 2013. Fluctuations of tidewater glaciers in Hornsund Fjord (Southern Svalbard) since the beginning of the 20th century. Polish Polar Res. 34, 327—352. https://doi.org/10.2478/popore

Cabedo-Sanz, P., Belt, S.T., Knies, J., Husum, K., 2013. Identification of contrasting seasonal sea ice conditions during the Younger Dryas. Quaternary Sci. Rev. 79, 74—86. https://doi.org/10.1016/j.quascirev.2012.10.028

Campbell, J.W., Antoine, D., Armstrong, R., Arrigo, K., Balch, W., Barber, R., Behrenfeld, M., Bidigare, R., Bishop, J., Carr, M.E., Esaias, W., Falkowski, P., Hoepffner, N., Iverson, R., Kiefer, D., Lohrenz, S., Marra, J., Morel, A., Ryan, J., Vedernikov, V., Waters, K., Yentsch, C., Yoder, J., 2002. Comparison of algorithms for estimating ocean primary production from surface chlorophyll, temperature, and irradiance. Global Biogeochem. Cy. 16. https://doi.org/10.1029/2001gb001444

Carroll, M.L., Denisenko, S.G., Renaud, P.E., Ambrose, W.G., 2008. Benthic infauna of the seasonally ice-covered western Barents Sea: Patterns and relationships to environmental forcing. Deep-Sea Res. Pt. II 55, 2340—2351. https://doi.org/10.1016/j.dsr2.2008.05.022

Comiso, J.C., 2002. A rapidly declining perennial sea ice cover in the Arctic. Geophys. Res. Lett. 29, 2—5. https://doi.org/10.1029/2002GL015650

Cottier, F.R., Tverberg, V., Inall, M., Svendsen, H., Nilsen, F., Griffiths, C., 2005. Water mass modification in an Arctic fjord through cross-shelf exchange: The seasonal hydrography of Kongsfjorden, Svalbard. J. Geophys. Res.-Oceans 110, 1—18. https://doi.org/10.1029/2004JC002757

Curry, J.A., Schramm, J.L., Ebert, E.E. , 1995. Sea Ice-Albedo Climate Feedback Mechanism. J. Clim. 8, 240—247. https://doi.org/10.1175/1520-0442(1995)008⟨0240:SIACFM⟩2.0.CO;2

Dahlke, S., Hughes, N.E., Wagner, P.M., Gerland, S., Wawrzyniak, T., Ivanov, B., Maturilli, M., 2020. The observed recent surface air temperature development across Svalbard and concurring footprints in local sea ice cover. Int. J. Climatol. 40, 5246—5265. https://doi.org/10.1002/joc.6517

Dale, B., 2009. Eutrophication signals in the sedimentary record of dinoflagellate cysts in coastal waters. J. Sea Res. 61, 103—113. https://doi.org/10.1016/j.seares.2008.06.007

Dale, B., 1996. Dinoflagellate cyst ecology: modeling and geological applications. In: Jansonius, J., McGregor, D.C. (Eds.), Palynology: Principles and Applications. AASP Foundation, 1249—1275.

Dale, B., 1983. Dinoflagellate resting cysts: 'benthic plankton'. In: Fryxell, G.A. (Ed.), Survival Strategies of the Algae. Cambridge University Press, New York, 69—136.

Dale, B., 1976. Cyst formation, sedimentation, and preservation: Factors affecting dinoflagellate assemblages in recent sediments from Trondheimsfjord. Norway. Rev. Palaeobot. Palynol. 22, 39—60. https://doi.org/10.1016/0034-6667(76)90010-5

Dale, B., Dale, A.L., 2002. Environmental applications of dinoflagellate cysts and acritarchs. In: Haslett, S.K. (Ed.), Environmental Micropalaeontology. Arnold, London, 207—240.

Darling, K.F., Schweizer, M., Knudsen, K.L., Evans, K.M., Bird, C., Roberts, A., Filipsson, H.L., Kim, J.-H., Gudmundsson, G., Wade, C.M., Sayer, M.D.J., Austin, W.E.N., 2016. The genetic diversity, phylogeography and morphology of Elphidiidae (Foraminifera) in the Northeast Atlantic. Mar. Micropaleontol. 129, 1—23. https://doi.org/10.1016/j.marmicro.2016.09.001

de Vernal, A., Eynaud, F., Henry, M., Hillaire-Marcel, C., Londeix, L., Mangin, S., Matthiessen, J., Marret, F., Radi, T., Rochon, A., Solignac, S., Turon, J.-L., 2005. Reconstruction of sea-surface conditions at middle to high latitudes of the Northern Hemisphere during the Last Glacial Maximum (LGM) based on dinoflagellate cyst assemblages. Quaternary Sci. Rev. 24, 897—924. https://doi.org/10.1016/j.quascirev.2004.06.014

de Vernal, A., Henry, M., Matthiessen, J., Mudie, P.J., Rochon, A., Boessenkool, K.P., Eynaud, F., Grøsfjeld, K., Guiot, J., Hamel, D., Harland, R., Head, M.J., Kunz-Pirrung, M., Levac, E., Loucheur, V., Peyron, O., Pospelova, V., Radi, T., Turon, J.-L.,

Voronina, E., 2001. Dinoflagellate cyst assemblages as tracers of sea-surface conditions in the northern North Atlantic, Arctic and sub-Arctic seas: the new "n = 677" data base and its application for quantitative palaeoceanographic reconstruction. J. Quaternary Sci. 16, 681—698. https://doi.org/10.1002/jqs.659

de Vernal, A., Marret, F., 2007. Organic-Walled Dinoflagellate Cysts: Tracers of Sea-Surface Conditions. In: Hillaire-Marcel, C., de Vernal, A. (Eds.), Developments in Marine Geology, Elsevier. B.V., 371—408. https://doi.org/10.1016/S1572-5480(07)01014-7

de Vernal, A., Radi, T., Zaragosi, S., Van Nieuwenhove, N., Rochon, A., Allan, E., De Schepper, S., Eynaud, F., Head, M.J., Limoges, A., Londeix, L., Marret, F., Matthiessen, J., Penaud, A., Pospelova, V., Price, A., Richerol, T., 2020. Distribution of common modern dinoflagellate cyst taxa in surface sediments of the Northern Hemisphere in relation to environmental parameters: The new n=1968 database. Mar. Micropaleontol. 159, 101796. https://doi.org/10.1016/j.marmicro.2019.101796

de Vernal, A., Rochon, A., Fréchette, B., Henry, M., Radi, T., Solignac, S., 2013. Reconstructing past sea ice cover of the Northern Hemisphere from dinocyst assemblages: Status of the approach. Quaternary Sci. Rev. 79, 122—134. https://doi.org/10.1016/j.quascirev.2013.06.022

Dowdeswell, J.A., 1989. On the nature of Svalbard icebergs. J. Glaciol. 35, 224—234.

Dowdeswell, J.A., Drewry, D.J., 1985. Place Names on the Nordaustlandet Ice Caps, Svalbard. Polar Rec. (Gr. Brit). 22, 519—523. https://doi.org/10.1017/S0032247400005970

Dowdeswell, J.A., Ottesen, D., Evans, J., Cofaigh, C.Ó., Anderson, J.B., 2008. Submarine glacial landforms and rates of ice-stream collapse. Geology 36, 819—822. https://doi.org/10.1130/G24808A.1

Fensome, R.A., Taylor, F.J.R., Norris, G., Sarjeant, W.A.S., Wharton, D.I., Williams, G.L., 1993. A classification of fossil and living dinoflagellates. Micropaleontol. Spec. Publ. 7, 351.

Fer, I., Skogseth, R., Haugan, P.M., Jaccard, P., 2003. Observations of the Storfjorden overflow. Deep. Res. Part I Oceanogr. Res. Pap. 50, 1283—1303. https://doi.org/10.1016/S0967-0637(03)00124-9

Filipowicz, C., 1990. Textural parameters and classification of deposits in the modern glaciomarine environment, Hornsund Fjord, Spitsbergen. Acta Geol. Pol. 40, 29—67.

Fossile, E., Nardelli, M.P., Howa, H., Baltzer, A., Poprawski, Y., Baneschi, I., Doveri, M., Mojtahid, M., 2022. Influence of modern environmental gradients on foraminiferal faunas in the inner Kongsfjorden (Svalbard). Mar. Micropaleontol. 173, 19. https://doi.org/10.1016/j.marmicro.2022.102117

Fossile, E., Pia Nardelli, M., Jouini, A., Lansard, B., Pusceddu, A., Moccia, D., Michel, E., Péron, O., Howa, H., Mojtahid, M., 2020. Benthic foraminifera as tracers of brine production in the Storfjorden "sea ice factory". Biogeosciences 17, 1933—1953. https://doi.org/10.5194/bg-17-1933-2020

Glud, R.N., Holby, O., Hoffmann, F., Canfield, D.E., 1998. Benthic mineralization and exchange in Arctic sediments (Svalbard, Norway). Mar. Ecol. Prog. Ser. 173, 237—251.

Grøsfjeld, K., Harland, R., Howe, J., 2009. Dinoflagellate cyst assemblages inshore and offshore Svalbard reflecting their modern hydrography and climate. Norw. J. Geol. 89, 121—134.

Haarpaintner, J., Gascard, J.-C., Haugan, P.M., 2001. Ice production and brine formation in Storfjorden, Svalbard. J. Geophys. Res.-Oceans 106, 14001—14013. https://doi.org/10.1029/1999JC000133

Hagen, J.O., Liestøl, O., Roland, E., 1993. Glacier atlas of Svalbard and Jan Mayen. Nor. Polarinsitutt Meddelelser 129, 141.

Hald, M., Dahlgren, T., Olsen, T.-E., Lebesbye, E., 2001. Late Holocene palaeoceanography in Van Mijenfjorden, Svalbard. Polar Res. 20, 23—35. https://doi.org/10.3402/polar.v20i1.6497

Hald, M., Korsun, S., 1997. Distribution of modern benthic foraminifera from fjords of Svalbard, European Arctic. J. Foraminifer. Res. 27, 101—122. https://doi.org/10.2113/gsjfr.27.2.101

Hald, M., Steinsund, P.I., 1992. Distribution of surface sediment benthic Foraminifera in the southwestern Barents Sea. J. Foraminifer. Res. 22, 347—362. https://doi.org/10.2113/gsjfr.22.4.347

Hansen, A., Knudsen, K.L., 1995. Recent foraminiferal distribution in Freemansundet and Early Holocene stratigraphy on Edgeøya, Svalbard. Polar Res. 14, 215—238. https://doi.org/10.1111/j.1751-8369.1995.tb00690.x

Harland, R., 1982. Recent dinoflagellate cyst assemblages from the Southern Barents Sea. Palynology 6, 9—18. https://doi.org/10.1080/01916122.1982.9989231

Hayward, B.W., Coze, F.Le, Vandepitte, L., Vanhoorne, B., 2020. Foraminifera in the World Register of Marine Species (WoRMS) Taxonomic Database. J. Foraminifer. Res. 50, 291—300. https://doi.org/10.2113/gsjfr.50.3.291

Head, M.J., Harland, R., Matthiessen, J., 2001. Cold marine indicators of the late Quaternary: The new dinoflagellate cyst genus Islandinium and related morphotypes. J. Quaternary Sci. 16, 621—636. https://doi.org/10.1002/jqs.657

Hebbeln, D., Wefer, G., 1991. Effects of ice coverage and ice-rafted material on sedimentation in the Fram Strait. Nature 350, 409—411. https://doi.org/10.1038/350409a0

Heikkilä, M., Pospelova, V., Forest, A., Stern, G.A., Fortier, L., Macdonald, R.W., 2016. Dinoflagellate cyst production over an annual cycle in seasonally ice-covered Hudson Bay. Mar. Micropaleontol. 125, 1—24. https://doi.org/10.1016/j.marmicro.2016.02.005

Heikkilä, M., Pospelova, V., Hochheim, K.P., Kuzyk, Z.Z.A., Stern, G.A., Barber, D.G., Macdonald, R.W., 2014. Surface sediment dinoflagellate cysts from the Hudson Bay system and their relation to freshwater and nutrient cycling. Mar. Micropaleontol. 106, 79—109. https://doi.org/10.1016/j.marmicro.2013.12.002

Howe, J.A., Harland, R., Cottier, F.R., Brand, T., Willis, K.J., Berge, J.R., Grøsfjeld, K., Eriksson, A., 2010. Dinoflagellate cysts as proxies for palaeoceanographic conditions in Arctic fjords. In: Howe, J.A., Austin, W.E.N., Forwick, M., Paetzel, M. (Eds.), Fjord Systems and Archives. Geological Society, London, 61—74. https://doi.org/10.1144/SP344.6

Husum, K., Hald, M., 2004. Modern foraminiferal distribution in the subarctic Malangen fjord and adjoining shelf, Northern Norway. J. Foramin. Res. 34, 34—48. https://doi.org/10.2113/0340034

Jacobson, D.M., Anderson, D.M., 1996. Widespread phagocytosis of ciliates and other protists by marine mixotrophic and heterotrophic thecate dinoflagellates. J. Phycol. 32, 279—285. https://doi.org/10.1111/j.0022-3646.1996.00279.x

Javaux, E.J., Scott, D.B., 2003. Illustration of Modern Benthic Foraminifera from Bermuda and Remarks on Distribution in other Subtropical/Tropical Areas. Palaentologia Electronica 6, 29 pp.

Jennings, A.E., Weiner, N.J., Helgadottir, G., Andrews, J.T., 2004. Modern Foraminiferal Faunas of the Southwestern To Northern Iceland Shelf: Oceanographic and Environmental Controls. J. Foramin. Res. 34, 180—207. https://doi.org/10.2113/34.3.180

Jeong, H.J., 1999. The ecological roles of heterotrophic dinoflagellates in marine planktonic community. J. Eukaryot. Microbiol. 46, 390—396. https://doi.org/10.1111/j.1550-7408.1999.tb04618.x

Jernas, P., Klitgaard-Kristensen, D., Husum, K., Koç, N., Tverberg, V., Loubere, P., Prins, M., Dijkstra, N., Gluchowska, M., 2018. Annual changes in Arctic fjord environment and modern benthic foraminiferal fauna: Evidence from Kongsfjorden, Svalbard. Glob. Planet. Change 163, 119—140. https://doi.org/10.1016/j.gloplacha.2017.11.013

Jima, M., Jayachandran, P.R., Bijoy Nandan, S., Krishnapriya, P.P., Aswathy, N.K., Krishnan, K.P., Harikrishnan, M., Radhakrishnan, C.K., 2021. Stable isotopic signatures of sediment carbon and nitrogen sources and its relation to benthic meiofaunal distribution in the Arctic Kongsfjord. Mar. Ecol. 42, 1—11. https://doi.org/10.1111/maec.12648

Klitgaard-Kristensen, D., Sejrup, H.P., 1996. Modern benthic foraminiferal biofacies across the Northern North Sea. Sarsia 81, 97—106. https://doi.org/10.1080/00364827.1996.10413615

Korsun, S., Hald, M., 2000. Seasonal dynamics of benthic foraminifera in a glacially fed fjord of Svalbard, European arctic. J. Foramin. Res. 30, 251—271. https://doi.org/10.2113/0300251

Korsun, S., Pogodina, I.A., Forman, S.L., Lubinski, D.J., 1995. Recent foraminifera in glaciomarine sediments from three arctic fjords of Novaja Zemlja and Svalbard. Polar Res. 14, 15—32. https://doi.org/10.1111/j.1751-8369.1995.tb00707.x

Kowalewski, W., Rudowski, S., Zalewski, S.M., 1990. Seismoacoustic studies within Wijdefjorden, Spitsbergen. Polish Polar Res. 11, 287—300.

Kucharska, M., Kujawa, A., Pawłowska, J., Łącka, M., Szymańska, N., Lønne, O.J., Zajączkowski, M., 2019. Seasonal changes in foraminiferal assemblages along environmental gradients in Adventfjorden (West Spitsbergen). Polar Biol. 42, 569—580. https://doi.org/10.1007/s00300-018-02453-5

Kujawa, A., Łącka, M., Szymańska, N., Pawłowska, J., Telesiński, M.M., Zajączkowski, M., 2021. Could Norwegian fjords serve as an analogue for the future of the Svalbard fjords? State and fate of high latitude fjords in the face of progressive "atlantification". Polar Biol. 44, 2217—2233. https://doi.org/10.1007/s00300-021-02951-z

Kunz-Pirrung, M., 1998. Rekonstruktion der Oberflächenwassermassen der östlichen Laptevsee im Holozän anhand von aquatischen Palynomorphen. Berichte zur Polarforsch 281, 1—117.

Lepš, J., Šmilauer, P., 2003. Multivariate analysis of ecological data using CanocoTM. Cambridge University Press, Cambridge, UK.

Leu, E., Søreide, J.E., Hessen, D.O., Falk-Petersen, S., Berge, J., 2011. Consequences of changing sea-ice cover for primary and secondary producers in the European Arctic shelf seas: Timing, quantity, and quality. Prog. Oceanogr. 90, 18—32. https://doi.org/10.1016/j.pocean.2011.02.004

Loeblich Jr., A.R., Tappan, H., 1987. Foraminiferal Genera and their Classification. Van Nostrand Reinhold Company, New York.

Loeng, H., Ozhigin, V., Ådlandsvik, B., 1997. Water fluxes through the Barents Sea. ICES J. Mar. Sci. 54, 310—317. https://doi.org/10.1006/jmsc.1996.0165

Łącka, M., Zajączkowski, M., 2016. Does the recent pool of benthic foraminiferal tests in fjordic surface sediments reflect interannual environmental changes? The resolution limit of the foraminiferal record. Ann. Soc. Geol. Pol. 86, 59—71. https://doi.org/10.14241/asgp.2015.019

Mackensen, A., Schmiedl, G., Thiele, J., Damm, E., 2017. Microhabitat preferences of live benthic foraminifera and stable carbon isotopes off SW Svalbard in the presence of widespread methane seepage. Mar. Micropaleontol. 132, 1—17. https://doi.org/10.1016/j.marmicro.2017.04.004

Majewski, W., Szczuciński, W., Zajączkowski, M., 2009. Interactions of Arctic and Atlantic water-masses and associated environmental changes during the last millennium, Hornsund (SW Svalbard). Boreas 38, 529—544. https://doi.org/10.1111/j.1502-3885.2009.00091.x

Majewski, W., Zajączkowski, M., 2007. Benthic foraminifera in Adventfjorden, Svalbard: Last 50 years of local hydrograpic changes. J. Foramin. Res. 37, 107—124. https://doi.org/10.2113/gsjfr.37.2.107

Manley, T.O., 1995. Branching of Atlantic Water within the Greenland-Spitsbergen Passage: An estimate of recirculation. J. Geophys. Res. 100. https://doi.org/10.1029/95JC01251, 20,627-20,634

Marret, F., Bradley, L., de Vernal, A., Hardy, W., Kim, S.Y., Mudie, P.J., Penaud, A., Pospelova, V., Price, A.M., Radi, T., Rochon, A., 2020. From bi-polar to regional distribution of modern dinoflagellate cysts, an overview of their biogeography. Mar. Micropaleontol. 159, 101753. https://doi.org/10.1016/j.marmicro.2019.101753

Maslowski, W., Marble, D., Walczowski, W., Schauer, U., Clement, J.L., Semtner, A.J., 2004. On climatological mass, heat, and salt transports through the Barents Sea and Fram Strait from a pan-Arctic coupled ice-ocean model simulation. J. Geophys. Res. 109, C03032. https://doi.org/10.1029/2001jc001039

Matthiessen, J., de Vernal, A., Head, M.J., Okolodkov, Y., Zonneveld, K.A.F., Harland, R., 2005. Modem organic-walled dinoflagellate cysts in Arctic marine environments and their (paleo-) environmental significance. Paläontologische Zeitschrift 79, 3—51. https://doi.org/10.1007/bf03021752

Mertens, K.N., Price, A.M., Pospelova, V., 2012a. Determining the absolute abundance of dinoflagellate cysts in recent marine sediments II: Further tests of the *Lycopodium* marker-grain method. Rev. Palaeobot. Palyno. 184, 74—81. https://doi.org/10.1016/j.revpalbo.2012.06.012

Mertens, K.N., Rengefors, K., Moestrup, Ø., Ellegaard, M., 2012b. A review of recent freshwater dinoflagellate cysts: Taxonomy, phylogeny, ecology and palaeocology. Phycologia 51, 612—619. https://doi.org/10.2216/11-89.1

Mertens, K.N., Takano, Y., Gu, H., Yamaguchi, A., Pospelova, V., Ellegaard, M., Matsuoka, K., 2015. Cyst-theca relationship of a new dinoflagellate with a spiny round brown cyst, *Protoperidinium lewisiae* sp. nov., and its comparison to the cyst of *Oblea acanthocysta*. Phycol. Res. 63, 110—124. https://doi.org/10.1111/pre.12083

Mertens, K.N., Verhoeven, K., Verleye, T., Louwye, S., Amorim, A., Ribeiro, S., Deaf, A.S., Harding, I.C., De Schepper, S., González, C., Kodrans-Nsiah, M., De Vernal, A., Henry, M., Radi, T., Dybkjaer, K., Poulsen, N.E., Feist-Burkhardt, S., Chitolie, J., Heilmann-Clausen, C., Londeix, L., Turon, J.L., Marret, F., Matthiessen, J., McCarthy, F.M.G., Prasad, V., Pospelova, V., Kyffin Hughes, J.E., Riding, J.B., Rochon, A., Sangiorgi, F., Welters, N., Sinclair, N., Thun, C., Soliman, A., Van Nieuwenhove, N., Vink, A., Young, M., 2009. Determining the absolute abundance of dinoflagellate cysts in recent marine sediments: The *Lycopodium* marker-grain method put to the test. Rev. Palaeobot. Palyno. 157, 238—252. https://doi.org/10.1016/j.revpalbo.2009.05.004

Mertens, K.N., Yamaguchi, A., Takano, Y., Pospelova, V., Head, M.J., Radi, T., Pieńkowski, A.J., De Vernal, A., Kawami, H., Matsuoka, K., 2013. A new heterotrophic dinoflagellate from the north-eastern pacific, *Protoperidinium fukuyoi*: Cyst-theca relationship, phylogeny, distribution and ecology. J. Eukaryot. Microbiol. 60, 545—563. https://doi.org/10.1111/jeu.12058

Moestrup, Ø., Lindberg, K., Daugbjerg, N., 2009. Studies on woloszynskioid dinoflagellates IV: The genus *Biecheleria* gen. nov. Phycol. Res. 57, 203—220. https://doi.org/10.1111/j.1440-1835.2009.00540.x

Montresor, M., Lovejoy, C., Orsini, L., Procaccini, G., Roy, S., 2003. Bipolar distribution of the cyst-forming dinoflagellate *Polarella glacialis*. Polar Biol. 26, 186—194. https://doi.org/10.1007/s00300-002-0473-9

Montresor, M., Procaccini, G., Stoecker, D.K., 1999. *Polarella glacialis*, gen. nov., sp. nov. (Dinophyceae): Suessiaceae are still alive!. J. Phycol. 35, 186—197.

Mudie, P.J., Rochon, A., 2001. Distribution of dinoflagellate cysts in the Canadian Arctic marine region. J. Quaternary Sci. 16, 603—620. https://doi.org/10.1002/jqs.658

Murray, J.W., 1991. Ecology and Palaeoecology of Benthic Foraminifera. Longman Scientific and Technical.

Murray, J.W., Alve, E., 2016. Benthic foraminiferal biogeography in NW European fjords: A baseline for assessing future change. Estuar. Coast. Shelf Sci. 181, 218—230. https://doi.org/10.1016/j.ecss.2016.08.014

Müller, J., Wagner, A., Fahl, K., Stein, R., Prange, M., Lohmann, G., 2011. Towards quantitative sea ice reconstructions in the northern North Atlantic: A combined biomarker and numerical modelling approach. Earth Planet. Sci. Lett. 306, 137—148. https://doi.org/10.1016/j.epsl.2011.04.011

Nardelli, M.P., Fossile, E., Péron, O., Howa, H., Mojtahid, M., 2023. Early taphonomy of benthic foraminifera in Storfjorden 'sea-ice factory': the agglutinated/calcareous ratio as a proxy for brine persistence. Boreas 52, 109—123. https://doi.org/10.1111/bor.12592

Nilsen, F., Cottier, F.R., Skogseth, R., Mattsson, S., 2008. Fjord-shelf exchanges controlled by ice and brine production: The interannual variation of Atlantic Water in Isfjorden, Svalbard. Cont. Shelf Res. 28, 1838—1853. https://doi.org/10.1016/j.csr.2008.04.015

Nilsen, F., Skogseth, R., Vaardal-Lunde, J., Inall, M., 2016. A Simple Shelf Circulation Model: Intrusion of Atlantic Water on the West Spitsbergen Shelf. J. Phys. Oceanogr. 46, 1209—1230. https://doi.org/10.1175/JPO-D-15-0058.1

Nürnberg, D., Wollenburg, I., Dethleff, D., Eicken, H., Kassens, H., Letzig, T., Reimnitz, E., Thiede, J., 1994. Sediments in Arctic sea ice: Implications for entrainment, transport and release. Mar. Geol. 119, 185—214. https://doi.org/10.1016/0025-3227(94)90181-3

Obrezkova, M.S., Pospelova, V., Kolesnik, A.N., 2023. Diatom and dinoflagellate cyst distribution in surface sediments of the Chukchi Sea in relation to the upper water masses. Mar. Micropaleontol. 178, 102184. https://doi.org/10.1016/j.marmicro.2022.102184

Pawłowska, J., Łącka, M., Kucharska, M., Szymańska, N., Koziorowska, K., Kuliński, K., Zajączkowski, M., 2017. Benthic foraminifera contribution to fjord modern carbon pools: A seasonal study in Adventfjorden. Spitsbergen. Geobiology 15, 704—714. https://doi.org/10.1111/gbi.12242

Pfirman, S.L., Bauch, D., Gammelsrød, T., 1994. The Northern Barents Sea: Water Mass Distribution and Modification. In: Johannessen, O.M., Muench, R.D., Overland, J.E. (Eds.), The Polar Oceans and Their Role in Shaping the Global Environment, Vol. 85. American Geophysical Union, 77—94.

Polyak, L., Mikhailov, V., 1996. Post-glacial environments of the southeastern Barents Sea: foraminiferal evidence. Geol. Soc. London, Sp. Publ., Vol. 111, 323—337.

Pospelova, V., Chmura, G.L., Boothman, W.S., Latimer, J.S., 2005. Spatial distribution of modern dinoflagellate cysts in polluted estuarine sediments from Buzzards Bay (Massachusetts, USA) embayments. Mar. Ecol. Prog. Ser. 292, 23—40. https://doi.org/10.3354/meps292023

Pospelova, V., Esenkulova, S., Johannessen, S.C., O'Brien, M.C., Macdonald, R.W., 2010. Organic-walled dinoflagellate cyst production, composition and flux from 1996 to 1998 in the central Strait of Georgia (BC, Canada): A sediment trap study. Mar. Micropaleontol. 75, 17—37. https://doi.org/10.1016/j.marmicro.2010.02.003

Pospelova, V., Head, M.J., 2002. *Islandinium brevispinosum* sp. nov. (Dinoflagellata), a new organic-walled dinoflagellate cyst from modern estuarine sediments of New England (USA). J. Phycol. 38, 593—601. https://doi.org/10.1046/j.1529-8817.2002.01206.x

Ramseier, R.O., Garrity, C., Bauerfeind, E., Peinert, R., 1999. Sea-ice impact on long-term particle flux in the Greenland Sea's Is Odden-Nordbukta region, 1985—1996. J. Geophys. Res. 104, 5329—5343. https://doi.org/10.1029/1998jc900048

Rasmussen, T.L., Forwick, M., Mackensen, A., 2012. Reconstruction of inflow of Atlantic Water to Isfjorden, Svalbard during the Holocene: Correlation to climate and seasonality. Mar. Micropaleontol. 94—95, 80—90. https://doi.org/10.1016/j.marmicro.2013.03.011

Rochon, A., de Vernal, A., Turon, J.-L., Matthiessen, J., Head, M.J., 1999. Distribution of recent dinoflagellate cysts in surface sediments from the North Atlantic Ocean and adjacent seas in relation to sea-surface parameters. Am. Assoc. Stratigr. Palynol. Contrib. Ser. 35, 1—146.

Romano, E., Bergamin, L., Parise, M., 2022. Benthic Foraminifera as Environmental Indicators in Mediterranean Marine Caves: A Review. Geosciences 12, 42. https://doi.org/10.3390/geosciences12010042

Rudels, B., Friedrich, H.J., 2000. The Transformations of Atlantic Water in the Arctic Ocean and Their Significance for the Freshwater Budget. In: Lewis, E.L., Jones, E.P., Lemke, P., Prowse, T.D., Wadhams, P. (Eds.), The Freshwater Budget of the Arctic Ocean. Springer, Dordrecht, 503—532. https://doi.org/10.1007/978-94-011-4132-1_21

Rudels, B., Jones, E.P., Anderson, L.G., Kattner, G., 1994. On the Intermediate Depth Waters of the Arctic Ocean. In: Johannessen, O.M., Muench, R.D., Overland, J.E. (Eds.), The Polar Oceans and Their Role in Shaping the Global Environment, Vol. 85. American Geophysical Union, 33—46. https://doi.org/10.1029/gm085p0033

Sakshaug, E., 2004. Primary and Secondary Production in the Arctic Seas. In: Stein, R., Macdonald, R.W. (Eds.), The Organic Carbon Cycle in the Arctic Ocean. Springer, Berlin, Heidelberg, 57—81. https://doi.org/10.1007/978-3-642-18912-8_3

Saloranta, T.M., Svendsen, H., 2001. Across the Arctic front west of Spitsbergen: high-resolution CTD sections from 1998—2000. Polar Res. 20, 177—184. https://doi.org/10.1111/j.1751-8369.2001.tb00054.x

Schiermeier, Q., 2007. Polar research: The new face of the Arctic. Nature 446, 133—135. https://doi.org/10.1038/446133a

Scott, D.B., Schell, T., Rochon, A., Blasco, S., 2008. Benthic foraminifera in the surface sediments of the Beaufort Shelf and slope, Beaufort Sea, Canada: Applications and implications for past sea-ice conditions. J. Marine Syst. 74, 840—863. https://doi.org/10.1016/j.jmarsys.2008.01.008

Seidenkrantz, M.-S., 2013. Benthic foraminifera as palaeo sea-ice indicators in the subarctic realm — examples from the Labrador Sea-Baffin Bay region. Quaternary Sci. Rev. 79, 135—144. https://doi.org/10.1016/j.quascirev.2013.03.014

Serreze, M.C., Barry, R.G., 2011. Processes and impacts of Arctic amplification: A research synthesis. Global Planet. Change 77, 85—96. https://doi.org/10.1016/j.gloplacha.2011.03.004

Serreze, M.C., Francis, J.A., 2006. The Arctic amplification debate. Clim. Change 76, 241—264. https://doi.org/10.1007/s10584-005-9017-y

Skogseth, R., Haugan, P.M., Haarpaintner, J., 2004. Ice and brine production in Storfjorden from four winters of satellite and in situ observations and modeling. J. Geophys. Res.-Oceans 109, 1—15. https://doi.org/10.1029/2004JC002384

Skogseth, R., Haugan, P.M., Jakobsson, M., 2005. Watermass transformations in Storfjorden. Cont. Shelf Res. 25, 667—695. https://doi.org/10.1016/j.csr.2004.10.005

Ślubowska, M.A., Koç, N., Rasmussen, T.L., Klitgaard-Kristensen, D., 2005. Changes in the flow of Atlantic water into the Arctic Ocean since the last deglaciation: Evidence from the northern Svalbard continental margin, 80°N. Paleoceanography 20, 1—16. https://doi.org/10.1029/2005PA001141

Smith Jr., W.O., Baumann, M.E.M., Wilson, D.L., Aletsee, L., 1987. Phytoplankton Biomass and Productivity in the Marginal Ice Zone of the Fram Strait During Summer 1984. J. Geophys. Res. 92, 6777—6786. https://doi.org/10.1029/JC092iC07p06777

Søreide, J.E., Leu, E.V.A., Berge, J., Graeve, M., Falk-Petersen, S., 2010. Timing of blooms, algal food quality and Calanus glacialis reproduction and growth in a changing Arctic. Glob. Change Biol. 16, 3154—3163. https://doi.org/10.1111/j.1365-2486.2010.02175.x

Stoecker, D.K., 1999. Mixotrophy among dinoflagellates. J. Eukaryot. Microbiol. 46, 397—401. https://doi.org/10.1111/j.1550-7408.1999.tb04619.x

Svendsen, H., Beszczyńska-Möller, A., Hagen, J.O., Lefauconnier, B., Tverberg, V., Gerland, S., Ørbøk, J.B., Bischof, K., Papucci, C., Zajączkowski, M., Azzolini, R., Bruland, O., Wiencke, C., Winther, J.G., Dallmann, W., 2002. The physical environment of Kongsfjorden-Krossfjorden, and Arctic fjord system in Svalbard. Polar Res. 21, 133—166. https://doi.org/10.1111/j.1751-8369.2002.tb00072.x

Syvitski, J.P.M., Shaw, J., 1995. Sedimentology and Geomorphology of Fjords. In: Perillo, G.M.E. (Ed.), Geomorphology and Sedimentology of Estuaries. Developments in Sedimentology. Elsevier Science B.V., 113—178. https://doi.org/10.1016/S0070-4571(05)80025-1

Szymańska, N., Łącka, M., Koziorowska-Makuch, K., Kuliński, K., Pawłowska, J., Kujawa, A., Telesiński, M.M., Zajączkowski, M., 2021. Foraminifera-derived carbon contribution to sedimentary inorganic carbon pool: A case study from three Norwegian fjords. Geobiology 19, 631—641. https://doi.org/10.1111/gbi.12460

Taylor, F.J.R., 1987. The Biology of Dinoflagellates. Blackwell Scientific, Oxford.

Taylor, F.J.R., Hoppenrath, M., Saldarriaga, J.F., 2008. Dinoflagellate diversity and distribution. Biodiversity Conservation 17, 407—418. https://doi.org/10.1007/s10531-007-9258-3

ter Braak, C.J.F., Šmilauer, P., 2002. CANOCO Reference Manual and CanoDraw for Windows user's Guide. Software for Canonical Community Ordination.

Wall, D., Dale, B., 1966. Living Fossils" in Western Atlantic Plankton. Nature 211, 1025—1026. https://doi.org/10.1038/2111025a0

Wallace, M.I., Cottier, F.R., Berge, J., Tarling, G.A., Griffiths, C., Brierley, A.S., 2010. Comparison of zooplankton vertical migration in an ice-free and a seasonally ice-covered Arctic fjord: An insight into the influence of sea ice cover on zooplankton behavior. Limnol. Oceanogr. 55, 831—845. https://doi.org/10.4319/lo.2009.55.2.0831

Węsławski, J.M., Jankowski, A., Kwasniewski, S., Swerpel, S., Ryg, M., 1991. Summer hydrology and zooplankton in two Svalbard fiords. Polish Polar Res. 12, 445—460.

Włodarska-Kowalczuk, M., Pawłowska, J., Zajączkowski, M., 2013. Do foraminifera mirror diversity and distribution patterns of macrobenthic fauna in an Arctic glacial fjord? Mar. Micropaleontol. 103, 30—39. https://doi.org/10.1016/j.marmicro.2013.07.002

WMO, 2014. Sea Ice Nomenclature.

Yamashita, C., Omachi, C., Santarosa, A.C.A., Iwai, F.S., Araujo, B.D., Disaró, S.T., Alves Martins, M.V., Vicente, T.M., Taniguchi, N., Burone, L., Mahiques, M.M., Bícego, M.C., Figueira, R.C.L., Sousa, S.H.M., 2020. Living benthic foraminifera of Santos continental shelf, southeastern Brazilian continental margin (SW Atlantic): chlorophyll-a and particulate organic matter approach. J. Sediment. Environ. 5, 17—34. https://doi.org/10.1007/s43217-019-00001-7

Zajączkowski, M., Szczuciński, W., Plessen, B., Jernas, P.E., 2010. Benthic foraminifera in Hornsund, Svalbard: Implications for paleoenvironmental reconstructions. Polish Polar Res. 31, 349—375. https://doi.org/10.2478/v10183

Zajączkowski, M., Włodarska-Kowalczuk, M., 2007. Dynamic sedimentary environments of an Arctic glacier-fed river estuary (Adventfjorden, Svalbard). I. Flux, deposition, and sediment dynamics. Estuar. Coast. Shelf Sci. 74, 285—296. https://doi.org/10.1016/j.ecss.2007.04.015

Zgrundo, A., Wojtasik, B., Convey, P., Majewska, R., 2017. Diatom communities in the High Arctic aquatic habitats of northern Spitsbergen (Svalbard). Polar Biol. 40, 873—890. https://doi.org/10.1007/s00300-016-2014-y

Zonneveld, K.A.F., 1997. New species of organic walled dinoflagellate cysts from modern sediments of the Arabian Sea (Indian Ocean). Rev. Palaeobot. Palyno. 97, 319—337. https://doi.org/10.1016/S0034-6667(97)00002-X

Zonneveld, K.A.F., Marret, F., Versteegh, G.J.M., Bogus, K., Bonnet, S., Bouimetarhan, I., Crouch, E., de Vernal, A., Elshanawany, R., Edwards, L., Esper, O., Forke, S., Grøsfjeld, K., Henry, M., Holzwarth, U., Kielt, J.F., Kim, S.Y., Ladouceur, S., Ledu, D., Chen, L., Limoges, A., Londeix, L., Lu, S.H., Mahmoud, M.S., Marino, G., Matsuoka, K., Matthiessen, J., Mildenhal, D.C., Mudie, P.J., Neil, H.L., Pospelova, V., Qi, Y., Radi, T., Richerol, T., Rochon, A., Sangiorgi, F., Solignac, S., Turon, J.L., Verleye, T., Wang, Y., Wang, Z., Young, M., 2013. Atlas of modern dinoflagellate cyst distribution based on 2405 data points. Rev. Palaeobot. Palyno. 191, 1—197. https://doi.org/10.1016/j.revpalbo.2012.08.003

Zonneveld, K.A.F., Pospelova, V., 2015. A determination key for modern dinoflagellate cysts. Palynology 39, 387—409. https://doi.org/10.1080/01916122.2014.990115